OPTIMAL STABILIZATION AND TRAJECTORY TRACKING OF AN AUTONOMOUS UNDERWATER VEHICLE (AUV)

Submitted by:

OWAIS KAMAL
NUST201361578MPNEC45013F

Supervised by:
Dr. ATTAULLAH Y. MEMON

THESIS

Submitted to:

Department of Electronics and Power Engineering,

Pakistan Navy Engineering College Karachi,

National University of Science and Technology, Islamabad

In fulfillment of requirements for the award of the degree of

MASTER OF SCIENCE IN ELECTRICAL ENGINEERING

With Specialization in Control

August 2017

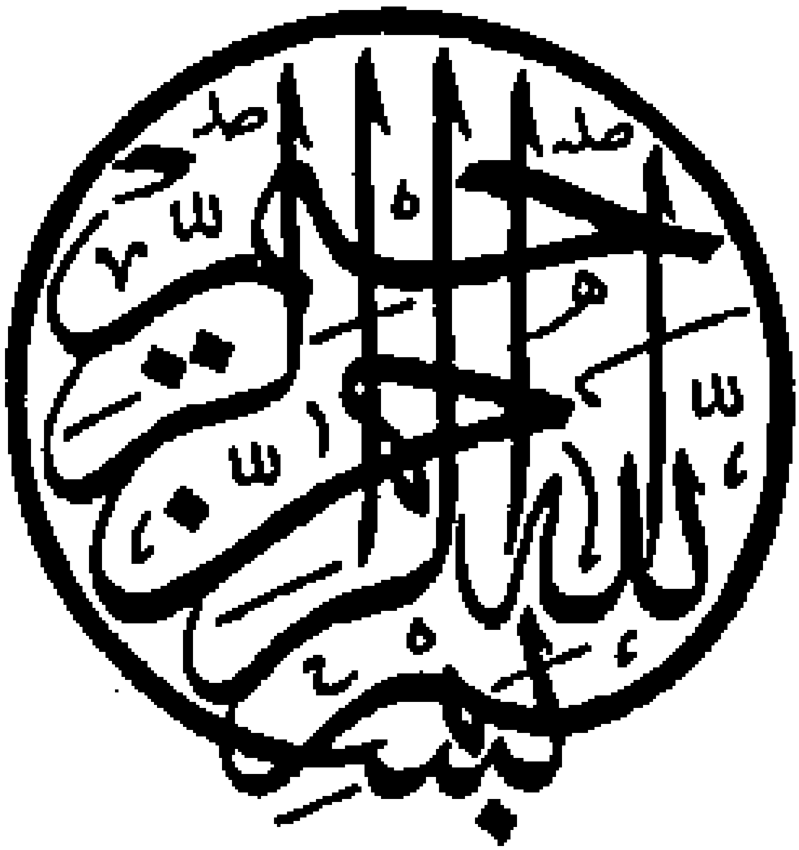
بسم الله الرحمن الرحيم

THESIS ACCEPTANCE CERTIFICATE

Certified that final copy of MS/MPhil thesis written by Mr Owais Kamal (Regn No. NUST201361578MPNEC45013F of PNEC (School/college/Institute) has been vetted by undersigned, found complete in all respects as per NUST Status/Regulations, is free of plagiarism, errors, and mistakes and is accepted as partial fulfillment for award of MS/MPhil degree. It is further certified that necessary amendments as pointed out by GEC members of the scholar have been incorporated in the said thesis.

Signature: ______________

Name of Supervisor Dr Attaullah Y Memon

Dated: 18-8-17

Signature: HoD______________

Dated: 21-8-17

Signature: (Dean/Principal):______________

Dated: 30/08/2017

Abstract

An optimal robust output feedback controller is proposed to stabilize a nonlinear, non-minimum phase system of an Autonomous Underwater Vehicle (AUV). Starting with a 6 DOF model of AUV, its motion is decoupled into diving and steering planes. The decoupled diving plane model of AUV is used to stabilize depth plane of AUV. This thesis aims to investigate performance of various control schemes and draws a comparison of their performance in a variety of operational scenarios. We begin by designing linear state feedback as well as output feedback controllers based on linearization and linear optimal control design methods. We then extend this linear control designs to include nonlinear dynamics and use nonlinear control design methods such as Sliding Mode Control and Inverse Optimal Control techniques to investigate the performance of the AUV system in presence of the parametric uncertainties. State feedback designs are extended to Output feedback designs using full-order and reduced-order High Gain Observers as appropriate. A thorough performance comparison of the various control schemes is presented with the help of mathematical analysis as well as simulations.

Acknowledgement

I am very much grateful to Almighty ALLAH, the most merciful and beneficent, whose ample blessings enable us to recognize and pursue knowledge in life. My sincere gratitude to my supervisor Dr. Attaullah Y. Memon, Department of Electronic and Power Engineering at PN Engineering College, NUST. I consider myself very lucky and honored to have him as my supervisor. I thank him for his unprecedented attention and patience throughout the thesis work. I admire him as a teacher and as a person.

In addition to above, I am also thankful to the guidance committee comprising of following faculty members who led me to achieve my target:

- Dr. Sajjad Haider Zaidi
- Dr. Aleem Mushtaq

I want to take this opportunity to thank my parents, my brother and sister, my aunts and my friends. Thank you for your prayers, love, encouragement, patience…Thank you for everything.

TABLE OF CONTENTS

List of Figures

List of Tables

List of Symbols and Abbreviations

SYMBOLS

J	Cost Function
δ	Delta Function
A	System Matrix
B	Input Matrix
C	Output Matrix
x_1	System State 1 (depth of AUV)
x_2	System State 2 (diving angle of AUV)
x_3	System State 3 (linear velocity of AUV in downward direction)
x_4	System State 4 (rate of change of angle)
u	Control input
δ_s	Control input (stern plane angle)
ρ'	Relative degree of the system
$\hat{\xi}_1, \hat{\xi}_2, \hat{\xi}_3, \hat{\xi}_4$	Estimated states from observer

h_1, h_2, h_3, h_4 Observer gains

ABBREVIATIONS

AUV Autonomous Underwater Vehicle

ARE Arithmetic Ricatti Equation

CLF Control Lyapunov Function

HGO High Gain Observer

HWT Heavy Weight Torpedo

LQG Linear Quadratic Gaussian

MIMO Multi-Input/Multi Output

PID Proportional-Integral-Derivative

REMUS Remote Environmental Monitoring Unit System

RHC Receding Horizon Control

SISO Single-Input/Single-Output

SMC Sliding Mode Control

SNAME Society of Naval Architecture and Marine Engineers

Chapter 1

INTRODUCTION

The optimal and robust control for nonlinear systems is a complex and challenging task in the field of control engineering. The optimal controls problem is recognized to be categorized as Hamilton-Jacobi-Bellman HJB Equations [1], [2], [3], [4]. Optimal performance value function is achieved by solving HJB equation. It determines under smooth conditions an optimal control. In most of the situations it is very difficult to have solution of HJB equations analytically because of its complexity. In this thesis, a dynamical nonlinear system of AUV is considered. Optimal stabilization of the system under consideration with robustness is the main task. Different control strategies are applied to get a reduced cost optimal and robust solution for the dynamical system stabilization.

1.1 Motivation

Optimized, cost efficient, robust and stabilized working of AUV is of great concern due to desired less consumption of fuel with uncertainties rejection capabilities, which in return allows a long and efficient trip. Reason for the selection of this topic is the importance of AUV's applications that requires long run time with stability. These applications include rescue operations, sea-floor mapping for building subsea infrastructure, oceanographic surveys etc.

Furthermore development of AUV's is necessary for ocean related civil applications like rescue operations. In military applications, it is used for sea border surveys, observing and reporting any expected alien intrusion. Therefore development of AUV's is an important national need.

This work shall investigate linear and non-linear optimal and robust stabilization of AUV to achieve the following goals:

- Fully stabilized system
- Cost and energy efficient control
- Robust control
- Uncertainties rejection capabilities in system states measurement

1.2 Objective of the Thesis

The primary objective of this research is to stabilize the nonlinear, non-minimum phase control system of an AUV using different linear, nonlinear control techniques and their comparison. Inverse Optimal Control based on Control Lyapunov Function (CLF). Following objectives are intended to be achieved:

- Understanding AUV's non-linear dynamics and their maneuvering.
- De-coupling equations of motion of the model in diving plane and designing of linear state-feedback and optimal controller for the nonlinear diving model of AUV with and without state estimator (observer).
- Designing of different nonlinear stabilizing controllers for optimal and robust stabilization of AUV with and without nonlinear state estimators (reduced and full order HGO).

- Simulating and comparing the results of AUV's system model in closed loop applying proposed controllers for its stabilization.

1.3 Literature Review

The linear and nonlinear coupled and decoupled dynamical models of AUV system were studied. The control strategies studied and used in this work includes state-feedback control, optimal control, SMC, lyapunov redesign and Inverse optimal control. The CLF based control design theory with past work will be presented that provides the stability results in this thesis. Optimal state feedback control will then be explained and the work done by researchers in its development will be discussed. Robust control technique, the SMC is then discussed. The state estimator technique HGO will be discussed.

1.3.1 Control Lyapunov Function

Asymptotic stability of equilibrium points of dynamical systems is analyzed using lyapunov functions [6], [7] and [8]. One of the most useful and successful Lyapunov methodology is its generalization to control systems designing and is known as Control Lyapunov Function (CLF) [9], [10] and [11]. For the stabilization of nonlinear dynamical systems with control inputs, CLF existence is a sufficient condition [11]. Different control laws can be calculated using CLF's, those can globally asymptotically stabilize the dynamical systems. For example in an Inverse optimal control technique, CLF is used to guarantee the globally asymptotically stabilization of the system but the cost functional minimized by the control is not specified before its solution. An important example of Inverse optimal control is Sontag's formula based on optimization problem solution using inverse optimal control [12]. In [13] a method is proposed to construct

CLF's for a given system. A control law is also designed and proposed based on Inverse optimal technique which is a generalization of Sontag's formula containing design parameter.

1.3.2 Inverse Optimal Control

Inverse Optimality provides information regarding a control law optimal with reference to some performance index. In [14] it was shown that with respect to some cost index, every control law is trivially optimal. The condition of being optimal is associated with some desirable properties if the there is any specific structure of cost index is the requirement. These results were generalized and extended in [15].For nonlinear system case in [16], and [17] it was shown that Inverse optimal control laws results in favorable gain margins. In some cases the large signal performance of the controller designed on the basis of CLF creates problem. In order to tackle this problem, the author in [18] reintroduced the inverse optimality approach in which firstly the controller is calculated and secondly it is proved as an optimal controller in relevance to a given significant cost function. Inverse optimal control ensures that the control effort applied on a dynamical system for its stabilization is not wasted.

Sontag's formula with respect to a meaningful cost function was shown to be optimal in [19]. A CLF based Inverse optimal control was presented in [20] that result in robustness to dynamic uncertainties of input. In [21] stabilization of a rigid aircraft using Inverse optimal control was explained whereas [22] explained the method of applying Inverse optimal control based on CLF calculated after system linearization.

1.3.3 Sliding Mode Control

SMC was developed and proposed in 1960's by Russian researchers. This technique becomes known internationally after the publication of book by Itkis [A] (1976) in English. After that, SMC become a general control method and is being used for different class of systems including SISO systems, MIMO systems, time variant systems, nonlinear systems etc. Due to its attractive features, SMC is used to control the dynamical systems having model uncertainties.

1.3.4 High Gain Observer (HGO)

HGO technique in nonlinear control systems started in 1980s by Saberi [23, 24], Tornambe [25], and Khalil [26]. In this context, two key papers, published in 1992, represent the beginning of two different types of research on HGO. The work presented by Gauthier [27] initiated a scope of work that is exemplified by [28–33]. This type of research covered a wide class of nonlinear systems and provided the results globally under the cases of global growth. The research work presented in [34] by Esfandiari and Khalil brought attention to the peaking phenomenon as an important feature of HGO. Although this phenomenon was observed earlier in [35, 36], the paper [34] explained that the interaction of peaking with nonlinearities could induce finite escape time. It also enlighten the destabilization drawback of HGO for a closed loop system in case of absence of global growth. It is due to the observer gain that could be driven sufficiently high. The designing of control to saturate in peaking interval is proposed to be global bounded function of the observed states of the dynamical system.

Soon afterwards, a number of well-known researchers in the field of nonlinear control systems started applying HGO's on nonlinear dynamical systems [36-41]. The researchers covered variety of problems associated with nonlinear control systems. This includes adaptive control, stabilization of the system, tracking desired trajectories of the system and regulation problems. They also explored how to use time-varying high-gain observers. For two decades Khalil with other researchers examine the applications of HGO's in the field of feedback control of nonlinear systems and addressing variety of problems [42–46].

Atassi & Khalil [47] proved a separation principle that adds up a novel dimension in results of Teel & Praly [27]; namely, the combination of control saturation with fast observer provides the controller with the output feedback to recover trajectories of the state feedback controller as gains of the observer chosen to be high.

In this work, output feedback controller having observer gains sufficiently high will be used in recovery of the trajectories of optimal state feedback controller.

1.4 Thesis Organization

The organization of the thesis comprises of five chapters.

Chapter 1: Gives the motivation behind Optimal and Robust Control of an AUV System, objectives of the thesis, literature review and the organization of the thesis.

Chapter 2: This chapter investigates the general nonlinear model of AUV. AUV's modeling (Kinematic and Dynamic) is taken into account. Transformation from earth fixed frame of reference to body fixed frame of reference is also used for simplification .Then that model is reduced to diving plane model by neglecting the unrelated parameters and forces. A type of AUV is also selected for reference calculations.

Chapter 3: In this chapter linear state-feedback control and optimal control is design and implemented on nonlinear model of AUV. Full order Observer is used in both of the control techniques to restore system's original measured states. Simulations are carried out to validate the quality of designed controllers and observers. Finally estimation of the region of attraction is calculated of AUV system states.

Chapter 4: This chapter includes the transformation of nonlinear system of AUV into input-output linearization normal form. Then nonlinear feedback stabilizing controller choosing suitable feedback gains is designed for stabilization of AUV. SMC is then designed to get a robust controller. The combined controller based on nonlinear stabilizing control and SMC is then designed. Optimal control is then calculated and another combined optimal robust controller is proposed having optimal and SMC controllers. Lyapunov redesign control technique is then used to reject any possible uncertainties in the input. Then Inverse optimal control is designed using a CLF guaranteeing global asymptotic stability to the system. Simulation results of all controllers are shown comparatively with their performances. Nonlinear reduced order observer HGO and full order HGO are used to estimate the un-measurable state and their validation through simulation are also incorporated in this chapter.

Chapter 5: This chapter highlights the conclusion of the thesis and recommendations for future work.

Chapter

2

THE AUTONOMOUS UNDERWATER VEHICLE SYSTEM

2.1 Introduction

In this chapter a nonlinear plant model of a general AUV system will be discussed and problem formulation will be presented. The nonlinear and linearized state space models of plant will be presented.

2.2 Overview of AUV System

The system under consideration is AUV system that is broadly considered in literature as a benchmark system for analyzing different control techniques [48], [49]. Since six DOF (Degree Of Freedom) are necessary to determine the orientation and position of AUV, this is a 6DOF system. Due to highly nonlinear dynamics, it is difficult for an underwater vehicle to stabilize itself under disturbances and gravitational and restoring forces. This makes it very challenging to control the nonlinear dynamics and hydrodynamics efficiently. There are generally three control inputs required to control this system. First control input is required in revolutions of propeller, which provides thrust to speed up the vehicle. This is the main source of movement of the vehicle. Then the control input required for angle of rudder to control the heading directions of the vehicle. Finally the control input required for angle of fins that regulates the diving of the vehicle.

2.3 Mathematical Modeling of AUV

Modeling of AUV system involves learning the dynamics of AUV and its statics. Statics includes the equilibrium of the vehicle in uniform velocity or at stationary position while dynamics deals with the accelerated motion of the vehicle. Dynamics is further sub-categorized in kinematics and kinetics. Kinematics deals with the vehicle motion's geometrical aspects whereas kinetics deals with forces that are responsible of motion of the AUV.

Modeling the submersible vehicles in 6 Degree Of Freedom (DOF) is based on their position and orientation frameworks as described in [49].

A 6 Degree Of Freedom AUV model is represented in Fig 2.1 with its related coordinates.

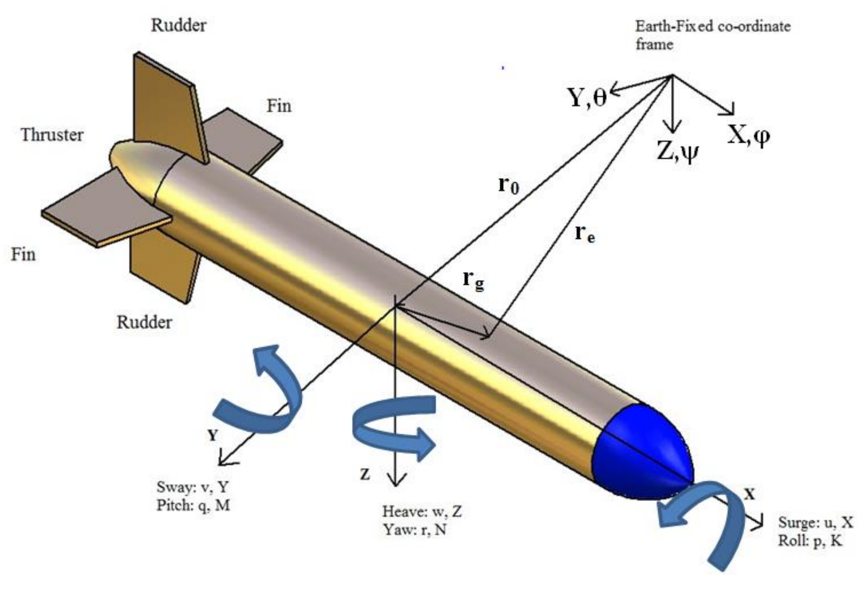

Figure2.1: Model of AUV in Earth and Body fixed frame of reference

Two frame of references, namely body fixed frame of reference and earth fixed frame of reference are used to explain 6 DOF AUV model. The earth fixed frame of reference describes the Euler angles and position of the AUV. Whereas the body fixed frame of reference describes linear and angular velocities related to AUV. Some important and useful notations used for marine vehicles motions and rotations are described in Table 1. These notations are used to better understand the AUV motions and rotations.

Table 1 Useful notations used for marine vehicles

DOF		**Axis**	**Positions and Euler angles**	**Linear and Angular Motions**	**Linear and angular velocities**
1st	Motions in	x	x	Surge	u
2nd		y	y	Sway	v
3rd		z	z	Heave	w
4th	Rotations about	x	∅	Roll	p
5th		y	θ	Pitch	q
6th		z	ψ	Yaw	r

In the above table 1, position and translational motion of AUV are described by the first coordinates & time derivatives. Whereas the last three coordinates are used to explain the orientation and rotational motion of AUV.

AUV motion is defined in body fixed coordinate system with reference to earth fixed coordinate system. Acceleration on point of earth surface is negligible in comparison with the inertial frame. Therefore earth fixed frame is considered as inertial frame. In order to have more simplifications 'η' is transformed from earth fixed frame to body fixed frame by using the following Jacobian transformation:

$$\dot{\eta} = J(\eta)v \tag{2.1}$$

Above shown equation is the velocity transformation that relates AUV flight path relative to inertial frame.

The kinematic equation of AUV is shown below:

$$\dot{\eta} = J(\eta)v = \begin{bmatrix} J_1(\eta_2) & 0_{3x3} \\ 0_{3x3} & J_2(\eta_2) \end{bmatrix} \begin{bmatrix} v_1 \\ v_2 \end{bmatrix} \tag{2.2}$$

Where $\eta \in R^{6x1}$ a vector in earth fixed coordinate system containing attitude and position of AUV,

$v \in R^{6x1}$ a vector in body fixed coordinate system containing linear velocities vector and angular velocities vector of AUV,

$v_1 = [u \quad v \quad \omega]^T$ a vector having linear velocities of AUV,

$v_2 = [p \quad q \quad r]^T$ a vector having angular velocities of AUV.

$J_1(\eta_2)$ defined as transformation matrix and is connected using different Euler angles functions,

$J_2(\eta_2)$ defined as transformation matrix that relates the 'v_2', the linear velocity vector with the euler rate vector η_2.

The dynamical model for AUV is derived from Newton and Euler equations of motion defined for rigid body inside liquid medium. Nonlinear dynamic equations of AUV can be stated as [49]:

$$M\dot{v} + C(v)v + D(v)v + g(\eta) = \tau \tag{2.3}$$

here,

M: is matrix having inertial terms

C(v): is matrix having coriolis and centripetal coefficients

D(v): Matrix with damping hydrodynamic terms

G(η): is buoyancy & gravity forces vector

v: is body fixed frame vector having velocity vectors v_1 and v_2 of AUV

η: Vector of inertial frame having position and altitude of AUV

$$\eta = [x \quad y \quad z \quad \phi \quad \theta \quad \psi]^T \tag{2.4}$$

here the positions of AUV are defined by x, y and z are and φ, θ and ψ are the orientations for the surge, sway, heave respectively.

And

$$v = [u \quad v \quad w \quad p \quad q \quad r]^T \tag{2.5}$$

where, ‘u’ denotes surge velocity, ‘v’ denotes sway velocity, ‘w’ denotes heave velocity, ‘p’ denotes roll velocity, ‘q’ denotes pitch velocity and ‘r’ denotes yaw velocity.

τ = Control input vector acting on AUV,

$$\tau = \left[f(\delta_\eta) \quad f(\delta_s) \quad f(n) \right]^T \tag{2.6}$$

where,

δ_η denotes the angle of diving plane

δ_s denotes the angle of the rudder

n denotes the revolution of the propeller

A nonlinear six DOF model of an AUV can be expressed by equations (2.1) and (2.3),

$$\begin{Bmatrix} \dot{\eta} = J(\eta)v \\ M\dot{v} + C(v)v + D(v)v + g(\eta) = \tau \end{Bmatrix} \tag{2.7}$$

Now state vector is defined as,

$$x(t) = [\eta(t) \quad v(t)]^T \tag{2.8}$$

2.4 Derivation of Equations in Diving Plane for AUV Motion

2.4.1 Mass and Inertial Matrix

The mass and inertial matrix in (2.3) can be represented,

$$M = M_{RB} + M_A \tag{2.9}$$

Here M_{RB} contains inertia related terms of the AUV rigid body and is considered as its actual mass. Whereas M_A have added inertia terms also known as virtual mass. This added mass inertia is actually moments and forces induced due to pressure produced by the in Diving Plane harmonic motion of the AUV and is related to the AUV's acceleration [49]. For a rigid body AUV, mass-inertia matrix is

$$M_{RB} = \begin{bmatrix} m & 0 & 0 & 0 & m z_G & -m y_G \\ 0 & m & 0 & -m z_G & 0 & m x_G \\ 0 & 0 & m & m y_G & -m x_G & 0 \\ 0 & -m z_G & m y_G & I_x & -I_{xy} & -I_{xx} \\ m z_G & 0 & -m x_G & -I_{yx} & I_y & -I_{yz} \\ -m y_G & m x_G & 0 & -I_{xx} & -I_{xy} & I_z \end{bmatrix} \tag{2.10}$$

The matrix of added mass inertia is

$$M_A = \begin{bmatrix} \frac{\partial X}{\partial \dot{u}} & \frac{\partial X}{\partial \dot{v}} & \frac{\partial X}{\partial \dot{w}} & \frac{\partial X}{\partial \dot{p}} & \frac{\partial X}{\partial \dot{q}} & \frac{\partial X}{\partial \dot{r}} \\ \frac{\partial Y}{\partial \dot{u}} & \frac{\partial Y}{\partial \dot{v}} & \frac{\partial Y}{\partial \dot{w}} & \frac{\partial Y}{\partial \dot{p}} & \frac{\partial Y}{\partial \dot{q}} & \frac{\partial Y}{\partial \dot{r}} \\ \frac{\partial Z}{\partial \dot{u}} & \frac{\partial Z}{\partial \dot{v}} & \frac{\partial Z}{\partial \dot{w}} & \frac{\partial Z}{\partial \dot{p}} & \frac{\partial Z}{\partial \dot{q}} & \frac{\partial Z}{\partial \dot{r}} \\ \frac{\partial K}{\partial \dot{u}} & \frac{\partial K}{\partial \dot{v}} & \frac{\partial K}{\partial \dot{w}} & \frac{\partial K}{\partial \dot{p}} & \frac{\partial K}{\partial \dot{q}} & \frac{\partial K}{\partial \dot{r}} \\ \frac{\partial M}{\partial \dot{u}} & \frac{\partial M}{\partial \dot{v}} & \frac{\partial M}{\partial \dot{w}} & \frac{\partial M}{\partial \dot{p}} & \frac{\partial M}{\partial \dot{q}} & \frac{\partial M}{\partial \dot{r}} \\ \frac{\partial N}{\partial \dot{u}} & \frac{\partial N}{\partial \dot{v}} & \frac{\partial N}{\partial \dot{w}} & \frac{\partial N}{\partial \dot{p}} & \frac{\partial N}{\partial \dot{q}} & \frac{\partial N}{\partial \dot{r}} \end{bmatrix} \tag{2.11}$$

As per notation used in SNAME [52],

$$X_{\dot{u}} = \frac{\partial X}{\partial \dot{u}} \;....\; and \;\; N_{\dot{r}} = \frac{\partial N}{\partial \dot{r}}$$

Now M_A can be written as

$$M_A = -\begin{bmatrix} X_{\dot{u}} & X_{\dot{v}} & X_{\dot{w}} & X_{\dot{p}} & X_{\dot{q}} & X_{\dot{r}} \\ Y_{\dot{u}} & Y_{\dot{v}} & Y_{\dot{w}} & Y_{\dot{p}} & Y_{\dot{q}} & Y_{\dot{r}} \\ Z_{\dot{u}} & Z_{\dot{v}} & Z_{\dot{w}} & Z_{\dot{p}} & Z_{\dot{q}} & Z_{\dot{r}} \\ K_{\dot{u}} & K_{\dot{v}} & K_{\dot{w}} & K_{\dot{p}} & K_{\dot{q}} & K_{\dot{r}} \\ M_{\dot{u}} & M_{\dot{v}} & M_{\dot{w}} & M_{\dot{p}} & M_{\dot{q}} & M_{\dot{r}} \\ N_{\dot{u}} & N_{\dot{v}} & N_{\dot{w}} & N_{\dot{p}} & N_{\dot{q}} & N_{\dot{r}} \end{bmatrix} \tag{2.12}$$

Now the total mass after adding the two matrices of added mass inertia and mass-inertia matrix of the rigid body gives

$$
M = \begin{bmatrix}
m - X_{\dot{u}} & -X_{\dot{v}} & -X_{\dot{w}} & -X_{\dot{p}} & m z_G - X_{\dot{p}} & -m y_G - X_{\dot{r}} \\
-Y_{\dot{u}} & m - Y_{\dot{v}} & -Y_{\dot{w}} & -m z_G - Y_{\dot{p}} & -Y_{\dot{q}} & m x_G - Y_{\dot{r}} \\
-Z_{\dot{u}} & -Z_{\dot{v}} & m - Z_{\dot{w}} & m y_G - Z_{\dot{p}} & -m x_G - Z_{\dot{q}} & -Z_{\dot{r}} \\
-K_{\dot{u}} & -m z_G - K_{\dot{v}} & m y_G - K_{\dot{w}} & I_x - K_{\dot{p}} & -I_{xy} - K_{\dot{q}} & -I_{xx} - K_{\dot{r}} \\
m z_G - M_{\dot{u}} & -M_{\dot{v}} & -m x_G - M_{\dot{w}} & -I_{yx} - M_{\dot{p}} & I_y - M_{\dot{q}} & -I_{yz} - M_{\dot{r}} \\
-m y_G - N_{\dot{u}} & m x_G - N_{\dot{v}} & -N_{\dot{w}} & -I_{xx} - N_{\dot{p}} & -I_{xy} - N_{\dot{q}} & I_z - N_{\dot{r}}
\end{bmatrix} \tag{2.13}
$$

2.4.2 Coriolis and Centripetal Force

The coriolis and centripetal terms matrix is defined as

$$
C = C_A + C_{RB} \tag{2.14}
$$

Here C_A is the matrix of added terms whereas C_{RB} have the coriolis and centripetal terms of AUV rigid body and they are given as

$$
C_{RB} = \begin{bmatrix}
0 & 0 & 0 & m(y_G q + z_G r) & -m(x_G q - w) & -m(x_G r + v) \\
0 & 0 & 0 & -m(y_G p + w) & m(z_G r + x_G p) & -m(y_G r - \mu) \\
0 & 0 & 0 & -m(z_G p - v) & -m(z_G q + \mu) & m(x_G p + y_G q) \\
-m(y_G q + z_G r) & m(y_G p + w) & m(z_G p - v) & 0 & -I_{yx} q - I_{xx} p + I_z r & I_{yz} r + I_{xy} p - I_y q \\
m(x_G q - w) & -m(z_G r + x_G p) & m(z_G q + \mu) & I_{yx} q + I_{xx} p - I_z r & 0 & -I_{xx} r - I_{xy} q + I_x p \\
m(x_G r + v) & m(y_G r - \mu) & -m(x_G p + y_G q) & -I_{yz} r - I_{xy} p + I_y q & I_{xx} r + I_{xy} q - I_x p & 0
\end{bmatrix}
$$
(2.15)

and

$$C_A = \begin{bmatrix} 0 & 0 & 0 & 0 & -\gamma_3 & \gamma_2 \\ 0 & 0 & 0 & \gamma_3 & 0 & -\gamma_1 \\ 0 & 0 & 0 & -\gamma_2 & \gamma_1 & 0 \\ 0 & -\gamma_3 & \gamma_2 & 0 & -\gamma_6 & \gamma_5 \\ \gamma_3 & 0 & -\gamma_1 & \gamma_6 & 0 & -\gamma_4 \\ -\gamma_2 & \gamma_1 & 0 & -\gamma_5 & \gamma_4 & 0 \end{bmatrix} \qquad (2.16)$$

Here,

$$\gamma_1 = X_{\dot{u}}u + X_{\dot{v}}v + X_{\dot{w}}w + X_{\dot{p}}p + X_{\dot{q}}q + X_{\dot{r}}r$$
$$\gamma_2 = X_{\dot{v}}u + Y_{\dot{v}}v + Y_{\dot{w}}w + Y_{\dot{p}}p + Y_{\dot{q}}q + Y_{\dot{r}}r$$
$$\gamma_3 = X_{\dot{w}}u + Y_{\dot{w}}v + Z_{\dot{w}}w + Z_{\dot{p}}p + Z_{\dot{q}}q + Z_{\dot{r}}r$$
$$\gamma_4 = X_{\dot{p}}u + Y_{\dot{p}}v + Z_{\dot{p}}w + K_{\dot{p}}p + K_{\dot{q}}q + M_{\dot{r}}r$$
$$\gamma_5 = X_{\dot{q}}u + Y_{\dot{q}}v + Z_{\dot{q}}w + K_{\dot{q}}p + M_{\dot{q}}q + M_{\dot{r}}r$$
$$\gamma_6 = X_{\dot{r}}u + Y_{\dot{r}}v + Z_{\dot{r}}w + K_{\dot{r}}p + M_{\dot{r}}q + N_{\dot{r}}r$$

Adding these two matrices yields C

$$C = \begin{bmatrix} 0 & 0 & 0 & m(y_G q + z_G r) & -m(x_G q - w) - \gamma_3 & -m(x_G r + v) + \gamma_2 \\ 0 & 0 & 0 & -m(y_G p + w) + \gamma_3 & m(z_G r + x_G p) & -m(y_G r - \mu) - \gamma_2 \\ 0 & 0 & 0 & -m(z_G p - v) - \gamma_2 & -m(z_G q + \mu) + \gamma_1 & m(x_G p + y_G q) \\ -m(y_G q + z_G r) & m(y_G p + w) - \gamma_3 & m(z_G p - v) + \gamma_2 & 0 & -I_{yx}q - I_{xx}p + I_z r - \gamma_6 & I_{yz}r + I_{xy}p - I_y q + \gamma_5 \\ m(x_G q - w) + \gamma_3 & -m(z_G r + x_G p) & m(z_G q + \mu) - \gamma_1 & I_{yx}q + I_{xx}p - I_z r + \gamma_6 & 0 & -I_{xx}r - I_{xy}q + I_x p - \gamma_4 \\ m(x_G r + v) - \gamma_2 & m(y_G r - \mu) + \gamma_1 & -m(x_G p + y_G q) & -I_{yz}r - I_{xy}p + I_y q - \gamma_5 & I_{xx}r + I_{xy}q - I_x p + \gamma_4 & 0 \end{bmatrix}$$

(2.17)

2.4.3 Hydrodynamic damping effect

The effect of hydrodynamic damping is severe in case of the movement of vehicle with high speed. Basically hydrodynamic damping consists of two main forces, namely drag and lift.

$$D = D_{lift} + D_{drag} \tag{2.18}$$

At lower speeds, the effect of lift force is negligible and it can be neglected. The remaining drag force consists of linear and nonlinear drag force given as,

$$D_{drag} = D_{linear} + D_{nonlinear} \tag{2.19}$$

Where

$$D_{linear} = \begin{bmatrix} X_u & 0 & 0 & 0 & 0 & 0 \\ 0 & Y_v & 0 & 0 & 0 & 0 \\ 0 & 0 & Z_w & 0 & 0 & 0 \\ 0 & 0 & 0 & K_p & 0 & 0 \\ 0 & 0 & 0 & 0 & M_q & 0 \\ 0 & 0 & 0 & 0 & 0 & N_r \end{bmatrix} \tag{2.20}$$

$$D_{nonlinear} = -\begin{bmatrix} X_{u|u|}|u| & 0 & 0 & 0 & 0 & 0 \\ 0 & Y_{v|v|}|v| & 0 & 0 & 0 & 0 \\ 0 & 0 & Z_{w|w|}|w| & 0 & 0 & 0 \\ 0 & 0 & 0 & K_{p|p|}|p| & 0 & 0 \\ 0 & 0 & 0 & 0 & M_{q|q|}|q| & 0 \\ 0 & 0 & 0 & 0 & 0 & N_{r|r|}|r| \end{bmatrix} \tag{2.21}$$

The hydrodynamic damping matrix can now be represented as,

$$D_{nonlinear} = -\begin{bmatrix} X_u - X_{u|u|}|u| & 0 & 0 & 0 & 0 & 0 \\ 0 & Y_v - Y_{v|v|}|v| & 0 & 0 & 0 & 0 \\ 0 & 0 & Z_w - Z_{w|w|}|w| & 0 & 0 & 0 \\ 0 & 0 & 0 & K_p - K_{p|p|}|p| & 0 & 0 \\ 0 & 0 & 0 & 0 & M_q - M_{q|q|}|q| & 0 \\ 0 & 0 & 0 & 0 & 0 & N_r - N_{r|r|}|r| \end{bmatrix} \quad (2.22)$$

2.4.4 Restoring Forces and Gravitational Moments

As per hydrodynamics, the restoring forces based upon buoyant and gravitational forces. Considering 'm' to be the mass of the submerged AUV, 'g' is the acceleration due to gravity, 'ρ' to be the fluid density and ∇ as the fluid's volume that AUV displaces. Expressions for weight & buoyancy are defined below respectively,

$$W = mg$$

$$B = \rho g \nabla$$

According to [52] SNAME, the vector of restoring forces and gravitational moments is given as

$$g(\eta) = \begin{bmatrix} (W - B)\sin\theta \\ -(W - B)\cos\theta\sin\phi \\ -(W - B)\cos\theta\cos\phi \\ -(y_G W - y_B B)\cos\theta\cos\phi + (z_G W - z_B B)\cos\theta\sin\phi \\ (z_G W - z_B B)\sin\theta + (x_G W - x_B B)\cos\theta\cos\phi \\ -(x_G W - x_B B)\cos\theta\sin\phi - (y_G W - y_B B)\sin\theta \end{bmatrix} \quad (2.23)$$

If the weight and buoyancy of an AUV are equal then the AUV is said to be neutrally buoyant. And if in addition the geometric center lies at the gravitational center of the AUV then the gravitational moments and restoring forces can be neglected.

2.4.5 Derivation of Dynamic and Kinematic Model of AUV

A generalized mathematical model of AUV is presented by Thor I. Fossen [49] as given below,

$$\dot{X} = f(x) + g(x)u$$
$$\dot{X} = \begin{bmatrix} -M^{-1}[C + D] & -M^{-1}G \\ J & 0 \end{bmatrix} X + \begin{bmatrix} -M^{-1} \\ 0 \end{bmatrix} u \tag{2.24}$$

The description of J is

$$J = \begin{bmatrix} J_1 & 0 \\ 0 & J_2 \end{bmatrix} \tag{2.25}$$

Where

$$J_1(\phi,\theta,\psi) = \begin{bmatrix} c\psi\, c\theta & -s\psi\, c\phi + c\psi\, s\theta\, s\phi & s\psi\, s\phi + c\psi\, c\phi\, s\theta \\ s\psi\, c\theta & c\psi\, c\phi + s\phi\, s\theta\, s\psi & -c\psi\, s\phi + s\theta\, s\psi\, c\phi \\ -s\theta & c\theta\, s\phi & c\theta\, c\phi \end{bmatrix} \tag{2.26}$$

And

$$J_2(\phi,\theta,\psi) = \begin{bmatrix} 1 & s\phi t\theta & c\phi t\theta \\ 0 & c\phi & -s\phi \\ 0 & \dfrac{s\phi}{c\theta} & \dfrac{c\phi}{c\theta} \end{bmatrix} \tag{2.27}$$

here trigonometric function **sin** is denoted by **'s'**, **cos** is denoted by **'c'** and **tan** is denoted by **'t'**.

Dynamic Model of AUV

Putting (2.13), (2.17), (2.22) and (2.23) in (2.24) provides 6 DOF nonlinear equations of motion for surge, sway, heave, roll, pitch and yaw as shown below respectively

$$m[\dot{u} - vr + wq] = X \tag{2.28}$$

$$m[\dot{v} + ur - wp] = Y \tag{2.29}$$

$$m[\dot{w} - uq + vp] = Z \tag{2.30}$$

$$I_x\dot{p} + (I_z - I_y)qr + I_{xy}(pr - \dot{q}) - I_{yz}(q^2 - r^2) - I_{xz}(pq + \dot{r}) = K \tag{2.31}$$

$$I_y\dot{q} + (I_z - I_x)pr - I_{xy}(qr + \dot{p}) + I_{yz}(pq - \dot{r}) + I_{xz}(p^2 - r^2) = M \tag{2.32}$$

$$I_z\dot{r} + (I_y - I_x)pq - I_{xy}(p^2 - q^2) - I_{yz}(pr + \dot{q}) + I_{xz}(qr - \dot{p}) = N \tag{2.33}$$

Kinematic Model

The Kinematic model of AUV is described in (2.1) as

$$\dot{\eta} = J(\eta)v$$

where J is the matrix of Kinematic transformation as defined in (2.25). Substituting values of $\eta\,(2.4),\ v\,(2.5),\ and\ \ J\,(2.25)$ in (2.1) yields,

$$\begin{bmatrix} \dot{x} \\ \dot{y} \\ \dot{z} \\ \dot{\phi} \\ \dot{\theta} \\ \dot{\psi} \end{bmatrix} = \begin{bmatrix} c\psi\, c\theta & -s\psi\, c\theta + c\psi\, s\theta\, s\phi & s\psi\, s\phi + c\psi\, c\theta\, s\theta & 0 & 0 & 0 \\ s\psi\, c\theta & c\psi\, c\phi + s\phi\, s\theta\, s\psi & -c\psi\, s\phi + s\theta\, s\psi\, c\phi & 0 & 0 & 0 \\ -s\theta & c\theta\, s\phi & c\theta\, c\phi & 0 & 0 & 0 \\ 0 & 0 & 0 & 1 & s\phi\, t\theta & c\phi\, t\theta \\ 0 & 0 & 0 & 0 & c\phi & -s\phi \\ 0 & 0 & 0 & 0 & \dfrac{s\phi}{c\theta} & \dfrac{c\phi}{c\theta} \end{bmatrix} \begin{bmatrix} u \\ v \\ w \\ p \\ q \\ r \end{bmatrix} \tag{2.34}$$

This results in the following kinematics equations of AUV

$$\dot{x} = u\cos\psi\,\cos\theta - v(\sin\psi\,\cos\phi + \cos\psi\,\sin\theta\sin\phi) + w(\sin\psi\,\sin\phi + \cos\psi\,\cos\phi\sin\theta) \tag{2.35}$$

$$\dot{y} = u\sin\psi\,\cos\theta + v(\cos\psi\,\cos\phi + \sin\phi\sin\theta\sin\psi) - w(\cos\psi\,\sin\phi + \sin\theta\sin\psi\,\cos\phi) \tag{2.36}$$

$$\dot{z} = -u\sin\theta + v\cos\theta\sin\phi + w\cos\theta\cos\phi \tag{2.37}$$

$$\dot{\phi} = p + q\sin\phi\tan\theta + r\cos\phi\tan\theta \tag{2.38}$$

$$\dot{\theta} = q\cos\phi - r\sin\phi \tag{2.39}$$

$$\dot{\psi} = q\frac{\sin\phi}{\cos\theta} + r\frac{\cos\phi}{\cos\theta} \tag{2.40}$$

2.5 AUV Model in Diving Plane

In order to derive the diving model of AUV, the terms related to diving plane of AUV are considered and the terms related to steering plane are not taken into consideration. Forward speed of the AUV i.e ‘u’ is taken to be constant having value of 2 m/s. Thus it can be state that for diving plane,

$$p = \phi = r = \psi = v = y = 0 \tag{2.41}$$

Simplifying the set of equations defined by the dynamic and kinematics model of AUV in (2.28)-(2.33) and (2.35)-(2.40) respectively, yields

$$\begin{aligned}
& m[\dot{w} - uq] = Z_{\dot{w}}\dot{w} - X_{\dot{u}}uq + Z_{w}w + Z_{q}q + Z_{\delta_\eta}\delta_\eta \\
& I_y\dot{q} = M_{\dot{q}}\dot{q} + M_{w}w + M_{q}q + M_{\delta_\eta}\delta_\eta \\
& \dot{z} = -u\sin\theta + w\cos\theta \\
& \dot{\theta} = q
\end{aligned} \tag{2.42}$$

In order to extract the nonlinear diving plane model of AUV, the set of equations (2.42) is solved for $\dot{z}, \dot{\theta}, \dot{w}\ and\ \dot{q}$

$$\begin{aligned}
& \dot{z} = w\cos\theta - u\sin\theta \\
& \dot{\theta} = q \\
& \dot{w} = \frac{Z_w}{m - Z_{\dot{w}}}w + \frac{mu - X_{\dot{u}}u + Z_q}{m - Z_{\dot{w}}}q + \frac{Z_{\delta_\eta}}{m - Z_{\dot{w}}}\delta_\eta \\
& \dot{q} = \frac{M_w}{I_y - M_{\dot{q}}}w + \frac{M_q}{I_y - M_{\dot{q}}}q + \frac{M_{\delta_\eta}}{I_y - M_{\dot{q}}}\delta\eta
\end{aligned} \tag{2.43}$$

2.6 Problem Formulation

The problem under consideration is the depth control and stabilization of nonlinear AUV system. The depth motion of AUV can be represented in X-Z plane as shown in figure 2.1. For this purpose, the nonlinear coupled dynamical model of AUV presented in (2.7) is decoupled in diving plane. For diving model, the position, linear and angular velocities of AUV and the external forces on it are neglected. In diving nonlinear model of AUV, the six DOF dynamical model in (2.7) reduced to (2.44) and resembles the diving model derived in (2.43),

$$\begin{Bmatrix} \dot{\eta}_d = J_d(\eta_d)v_d \\ M_d \dot{v}_d + C_d(v_d)v_d + D_d(v_d)v_d + g_d(\eta_d) = \tau_d \end{Bmatrix} \tag{2.44}$$

Where,

$\eta_d(t) = [z \quad \theta]^T$ is the inertial frame vector for diving plane having depth and diving angle.

$v_d(t) = [w \quad q]^T$ vector having velocity in downward direction and rate of change of diving angle.

The decoupled models of AUV with their control inputs and required quantities to be measured (linear velocities, position, angular velocities and Euler angles) are described below,

Table 2 Decoupled Models of AUV

S. No	Decoupled Model	Control Input	Required Quantities
1	Diving	$\delta_s(t)$	z(t), θ(t), w(t), q(t)
2	Steering	$\delta_r(t)$	v(t), r(t), ψ(t)
3	Speed	n(t)	u(t)

The forward speed ‘u’ is selected as constant.

Chapter 3 LINEAR CONTROL DESIGNS FOR AUV

3.1 Introduction

This chapter provides detail about developing a linear stabilizing state-feedback controller via linearization for nonlinear dynamical system. The nonlinear dynamical equations of motions are linearized at a selected point (origin) and the system's stability is investigated. A linear optimal controller is then designed so that quadratic index of the system can be minimized. Simulations of controller are also incorporated in this chapter.

3.2 Nonlinear Equation of Motions of AUV in Diving Plane

The nonlinear dynamical system equations reduced to diving plane model by neglecting the yaw and roll motion elements. For simplification purposes, it is considered that the AUV is travelling smoothly in forward direction deep from the surface and the angle of diving is assumed so small.

The vehicle experiences hydrostatic forces and moments resulted due to the combined effects of the buoyancy and weight of AUV. Rigid body dynamics equations of AUV are simplified for pure depth plane motion. The linear and angular velocities in roll and yaw motions are dropped out with the equations for out-of-plane AUV motion. It results the following set of state equations of fourth order for the diving model of AUV:

$$\begin{aligned}
\dot{x}_1 &= x_3 \cos x_2 - u \sin x_2 \\
\dot{x}_2 &= x_4 \\
\dot{x}_3 &= \frac{Z_w}{m - Z_{\dot{w}}} x_3 + \frac{mu - X_{\dot{u}} u + Z_q}{m - Z_{\dot{w}}} x_4 + \frac{Z_{uu\delta_s}}{m - Z_{\dot{w}}} \delta_s \\
\dot{x}_4 &= \frac{M_w}{I_y - M_{\dot{q}}} x_3 + \frac{M_q}{I_y - M_{\dot{q}}} x_4 + \frac{M_{uu\delta_s}}{I_y - M_{\dot{q}}} \delta_s
\end{aligned} \qquad (3.1)$$

The eq. (3.2) is of the standard nonlinear form $\dot{x} = f(x) + g(x)u$. The steady state forward velocity of AUV is represented as "u".

Here,

$$\begin{aligned}
x_1 &= Depth\ of\ AUV\ (m) \\
x_2 &= Diving\ angle\ of\ AUV\ (rad) \\
x_3 &= Linear\ velocity\ downward\ (m/s) \\
x_4 &= Diving\ angle\ changing\ rate\ (rad/s) \\
\delta_s &= Control\ Input\ Fins\ angle\ (rad)
\end{aligned}$$

The output of the system is $x_1 = Depth\ of\ AUV\ (m)$. The output equation of the system is $y = Cx$.

The eq.(3.1) can be written as,

$$\begin{aligned}
\dot{x}_1 &= x_3 \cos x_2 - u \sin x_2 \\
\dot{x}_2 &= x_4 \\
\dot{x}_3 &= A_{31} x_3 + A_{32} x_4 + B_{31} \delta_s \\
\dot{x}_4 &= A_{41} x_3 + A_{42} x_4 + B_{41} \delta_s
\end{aligned} \qquad (3.2)$$

The values of coefficients used in the above equation are explained in **Appendix-A2**.

3.3 Stabilization

In control systems, the term stabilization refers to stabilization of a dynamical system. Suppose it is to investigate the stabilization of a nonlinear system at origin. If all of the states of the system are stable at origin then the system under consideration is said to be stable at that point. The stability of a given system can be identified by investigating the eigenvalues of the system matrix A at the selected point. If the system matrix A has unstable eigenvalue then the rank of the controllability matrix needs to be check whether or not the system is controllable. For nonlinear systems, the system is first to be linearized at a specified point of interest. This will lead to stabilization via linearization.

3.4 System Analysis via Linearization

In control designing of a system, it is necessary to find whether the system is controllable or not. After finding the controllability, suitable controller can be designed and applied on the system to check the systems stability on application of the control input. For this purpose, the nonlinear diving model of AUV in is linearized at origin. The physical and hydrodynamic parameters used in calculations and in simulations are defined in **Appendix A.1**.

Hypothesis 1 *The pairs of matrices (A, B) & (A, C) are point-wise controllable also observable State Dependent Coefficients parameterization respectively for all values of x of dynamical model of AUV.*

Remark 1 A necessary test for the controllability condition defined in hypothesis 1 is to examine the solution of controllability matrix and finding its rank, that is

$$\hat{C}(A(x), B(x)) = \begin{bmatrix} B(x) & A(x)B(x) & \cdots & A^{n-1}(x)B(x) \end{bmatrix} \tag{3.4}$$

must have its rank equal to the rank of the AUV system matrix.

Similarly a necessary test for the observability condition defined in hypothesis 1 is checking the rank of the observability matrix, that is

$$\hat{O}(A, C) = \begin{bmatrix} C(x) & C(x)A(x) & \cdots & C(x)A^{n-1}(x) \end{bmatrix}^T \tag{3.5}$$

$$has\ rank(\hat{O}) = n \quad \forall x \in \mathbb{R}^n$$

It is supposed that the diving angle of AUV is so small i.e.

$$\sin x_2 \cong x_2$$
$$\cos x_2 \cong 1$$

Now system matrix A becomes,

$$A = \begin{bmatrix} 0 & -u & 1 & 0 \\ 0 & 0 & 0 & 1 \\ 0 & 0 & A_{31} & A_{32} \\ 0 & 0 & A_{41} & A_{42} \end{bmatrix} \tag{3.6}$$

And the input matrix B becomes,

$$B = \begin{bmatrix} 0 \\ 0 \\ B_{31} \\ B_{41} \end{bmatrix} \tag{3.7}$$

3.4.1 Controllability Test of AUV System

In order to examine linearized system's controllability, rank of the controllability matrix can be found using hypothesis 1,

$$\hat{C} = \begin{bmatrix} B & AB & A^2B & A^3B \end{bmatrix} \tag{3.8}$$

By using **ctrb(A,B)** command on MATLAB, the rank of the controllability matrix found to be '4' that is the same as of the system matrix A. So the linearized diving system of AUV is controllable.

3.4.2 Observablility Test of AUV System

In order to investigate linearized system's observability, calculation is carried out to find rank of observability matrix by hypothesis 1,

$$\hat{O} = \begin{bmatrix} C & CA & CA^2 & CA^3 \end{bmatrix}^T \tag{3.9}$$

where $C = [1 \quad 0 \quad 0 \quad 0]$

By using **obsv(A,C)** command on MATLAB, the rank found is '4', that is same as of the system matrix A. So the linearized diving system of AUV is observable.

3.5 Stabilization using Linear Control Design

Since the system under consideration is stable and controllable at origin, a full-state linear feedback controller will be designed using pole placement method to stabilize the dynamical system.

Assume that the single input system dynamics are given by

$$\begin{aligned} \dot{x} &= Ax + B\delta_s \\ y &= Cx \end{aligned} \tag{3.10}$$

It is assumed that a full state feedback controller of the form

$$\delta_s(x) = r - Fx \tag{3.11}$$

is used to change the dynamics of the system to desired performance. Reference signal is represented by ‘r’ and gain matrix is F of the order $\Re^{1x4}$ in this case. The problem under consideration is to stabilize the system at origin, therefore r=0. Now this controller is called “regulator” and becomes,

$$\delta_s(x) = -Fx \tag{3.12}$$

Here F= [F_1 F_2 F_3 F_4]

For the closed loop system dynamics, inserting (3.11) in (3.10),

$$\dot{x} = Ax + B(r - Fx) \tag{3.13}$$

Since r=0 in this case,

$$\dot{x} = (A - BF)x$$
$$\dot{x} = A_{cl}x \quad (3.14)$$

The gain matrix F is to be selected such that the closed loop gain matrix A_{cl} has the desired properties. One of the poles is at 0 making open loop system to be marginally stable; it is desired to shift it to left half plane on root locus plot. Closed loop system's poles are chosen to be placed at P = [-1 -2 -3 -4] in order to achieve this task.

Ackermann's formula is a useful technique to find the gain matrix F. It provides a formula to find gains of the matrix F for 4th order systems as,

$$F = [0 \quad 0 \quad 0 \quad 1]\hat{C}^{-1}\Phi_d(A) \quad (3.15)$$

where,

$$\hat{C} = \begin{bmatrix} B & AB & A^2B & A^3B \end{bmatrix} \quad (3.16)$$

$\Phi_d(A)$ is the closed loop poles characteristic equation and evaluated for s=A.

$$\Phi_d(s) = (s+1)(s+2)(s+3)(s+4)$$
$$\Phi_d(s) = s^4 + 10s^3 + 35s^2 + 50s + 24 \quad (3.17)$$

And $$\Phi_d(A) = A^4 + 10A^3 + 35A^2 + 50a + 24I \quad (3.18)$$

Solving (3.15) using (3.16) and (3.18) results gain matrix F,

$$F = [11.2 \quad 38.2 \quad 3.6 \quad 11.5] \tag{3.19}$$

Now the control input from (3.12) becomes,

$$\delta_s(x) = -11.2x_1 + 38.2x_2 - 3.6x_3 + 11.5x_4 \tag{3.20}$$

3.5.1 Simulations on MATLAB/Simulink

The control input of (3.20) is then applied on the nonlinear dynamical model of the AUV system on Simulink. The numerical values for the physical parameters and the hydrodynamics forces and moments are described in Appendix-A1. The systems state response on the application of linear state feedback control is shown in Figure 3.1 below.

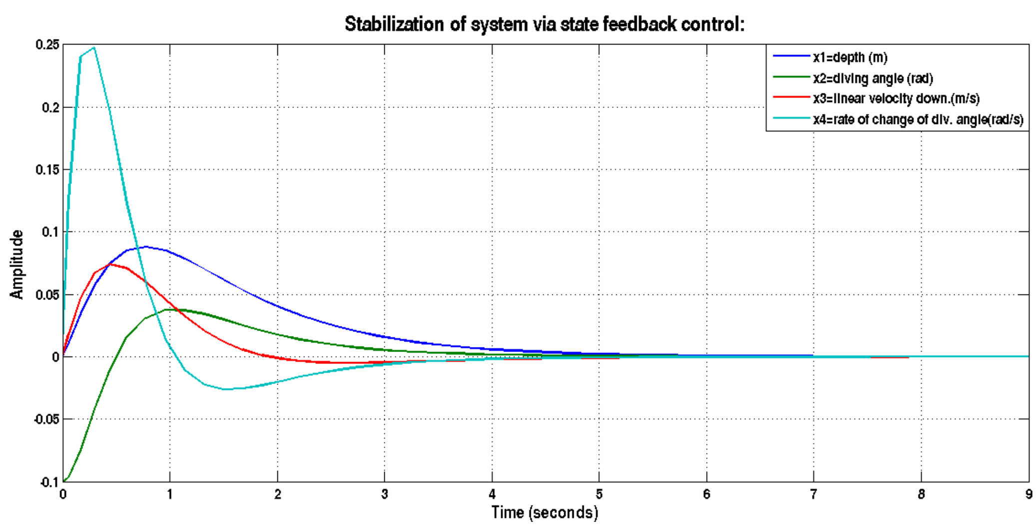

Figure 3.1: System response on application of linear state-feedback control

All of the systems states are going to stabilize on the application of linear state-feedback control after 7 seconds. It is observed that there is 0% error in the steady state of states and an overshoot of 25% in rate of change of angle with respect to the steady state is observed. The main aim of the stabilization via state feedback of nonlinear dynamical system is achieved.

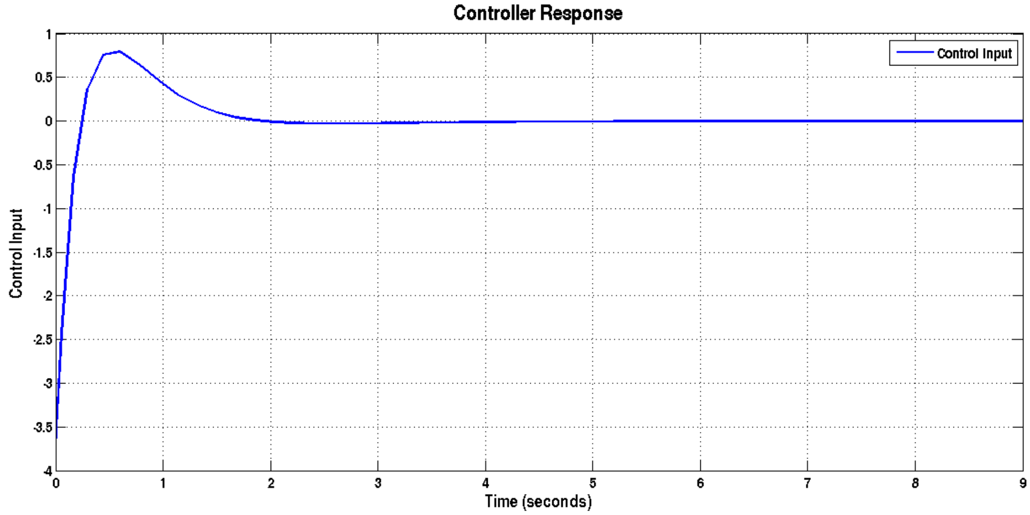

Figure 3.2: Linear state-feedback controller response

The linear state-feedback controller response is shown above in Figure 3.2. It is observed that the controller used more effort in first 5 seconds to stabilize the system.

3.6 Stabilization using Linear Control with Observer

The availability of all of the state variables all the time is the requirement of state feedback control for a system. Sometimes all of the states of the system to be controlled are not available for the measurements or they may not be practically measurable. The cost of the sensors to measure all of the system states can also be a serious restriction.

To eliminate these problems, one can estimate the states, creating additional dynamical system titled as observer, attached with AUV model. The main goal of an observer is the production of estimate of real system states.

Working on observer techniques is initiated by Luenberger in 1964. It is stated that a system that uses output of system under consideration as its input can work like observer for the considered system.

An observer has the basic structure of the system under consideration having two inputs and one output. These inputs include control input of system under consideration and its output. The output of an observer is the estimated states of original system.

Luenberger observer dynamics may better explained using equations below

$$\dot{\hat{x}} = A\hat{x} + Bu + K(y - C\hat{x}) \tag{3.21}$$

In the above expression observer gain is represented as 'K' whereas the the output prediction error is represented by $(y - C\hat{x})$. System error dynamics can be analyzed by $e = x - \hat{x}$. Now subtracting the observer dynamics from the plant dynamics

$\dot{e} = Ae + LC(x - \hat{x})$

$$\dot{e} = (A - LC)e \tag{3.22}$$

It has been verified in section 3.4.2 that the pair (A, C) is observable.

The basic structure of an observer with observer gain matrix ‘K’, and state-feedback controller gain ‘F’ is shown below:

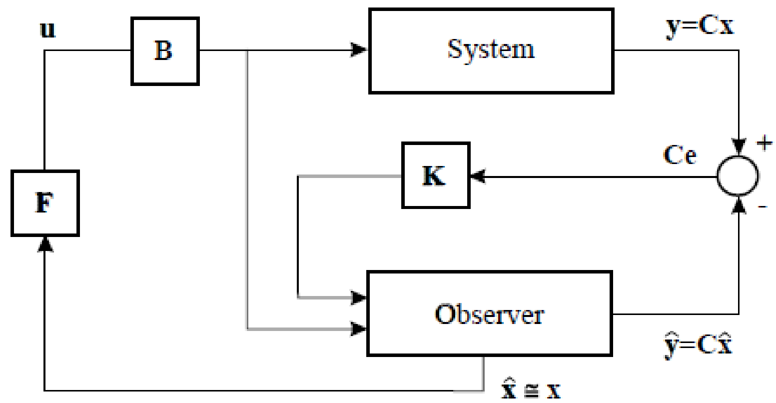

Figure 3.3 Basic Structure of an observer with state-feedback controller

In fig. (3.3), the observer gain ‘K’ is to be chosen such that the observation error is minimized.

Since the output of the system is depth that is the first state, its estimation error is given by $e_1 = x_1 - \hat{x}_1$. The observer output is represented by the following equations

$$\begin{aligned}
\dot{\hat{x}}_1 &= \hat{x}_3 - u\hat{x}_2 + L_1(x_1 - \hat{x}_1) \\
\dot{\hat{x}}_2 &= \hat{x}_4 + L_2(x_1 - \hat{x}_1) \\
\dot{\hat{x}}_3 &= A_{31}\hat{x}_3 + A_{32}\hat{x}_4 + B_{31}\delta_s + L_3(x_1 - \hat{x}_1) \\
\dot{\hat{x}}_4 &= A_{41}\hat{x}_3 + A_{42}\hat{x}_4 + B_{41}\delta_s + L_4(x_1 - \hat{x}_1)
\end{aligned} \tag{3.23}$$

The estimation offset in states of system & observer can be represented by $e_j = x_j - \hat{x}_j$ where j=1, 2, 3, 4. In the error coordinates, the closed loop system is

$$\begin{aligned}
\dot{e}_1 &= e_3 - u e_2 - L_1 e_1 \\
\dot{e}_2 &= e_4 - L_2 e_1 \\
\dot{e}_3 &= A_{31} e_3 + A_{32} e_4 - L_3 e_1 \\
\dot{e}_4 &= A_{41} e_3 + A_{42} e_4 - L_4 e_1
\end{aligned} \tag{3.24}$$

Now considering a lyapunov function,

$$V(e) = \sum \frac{1}{2} e_j^2 \tag{3.25}$$

Where j=1, 2, 3, 4. Differentiating V(e) w.r.t time

$$\dot{V}(e) = e_1\dot{e}_1 + e_2\dot{e}_2 + e_3\dot{e}_3 + e_4\dot{e}_4 \tag{3.26}$$

$$\dot{V}(e) = e_1(e_3 - u e_2 - L_1 e_1) + e_2(e_4 - L_2 e_1) + e_3(A_{31} e_3 + A_{32} e_4 - L_3 e_1) + e_4(A_{41} e_3 + A_{42} e_4 - L_4 e_1)$$

$$\begin{aligned}
\dot{V}(e) \le & -\left(L_1 - 1 - \frac{L_4}{2} - \frac{L_2}{2} - \frac{u}{2}\right)\left|e_1\right|^2 - \left(\frac{1}{2} - \frac{u}{2} - \frac{L_2}{2}\right)\left|e_2\right|^2 \\
& -\left(-A_{31} + \frac{1}{2}A_{32} - \frac{L_3}{2} + \frac{1}{2}A_{41} + \frac{1}{2}\right)\left|e_3\right|^2 - \left(-A_{42} + \frac{A_{32}}{2} - \frac{L_2}{2} + \frac{1}{2} + \frac{1}{2}A_{41}\right)\left|e_4\right|^2
\end{aligned}$$

The above inequality can also be written as,

$$\dot{V}(e) \le -\alpha_1\left|e_1\right|^2 - \alpha_2\left|e_2\right|^2 - \alpha_3\left|e_3\right|^2 - \alpha_4\left|e_4\right|^2 \tag{3.27}$$

In the above equation $\alpha_1, \alpha_2, \alpha_3 \; and \; \alpha_4$ are positive numbers that can be calculated by selecting suitable gains of observer i.e. $L_1, L_2, L_3 \; and \; L_4$ such that to achieve $\dot{V}(e) < 0$.

3.6.1 Simulations

For simulation purposes, the gain matrix K calculation is carried out with poles values $P = [-1.5 \quad -2.5 \quad -3.5 \quad -4.5]$ that yields the gain matrix $K = [10.1 \quad -24.3 \quad -13.7 \quad -30.7]$. Simulating the system with the feedback controller and observer, fig. (3.4) shows the effective state estimation of all the system states using only the output of the system.

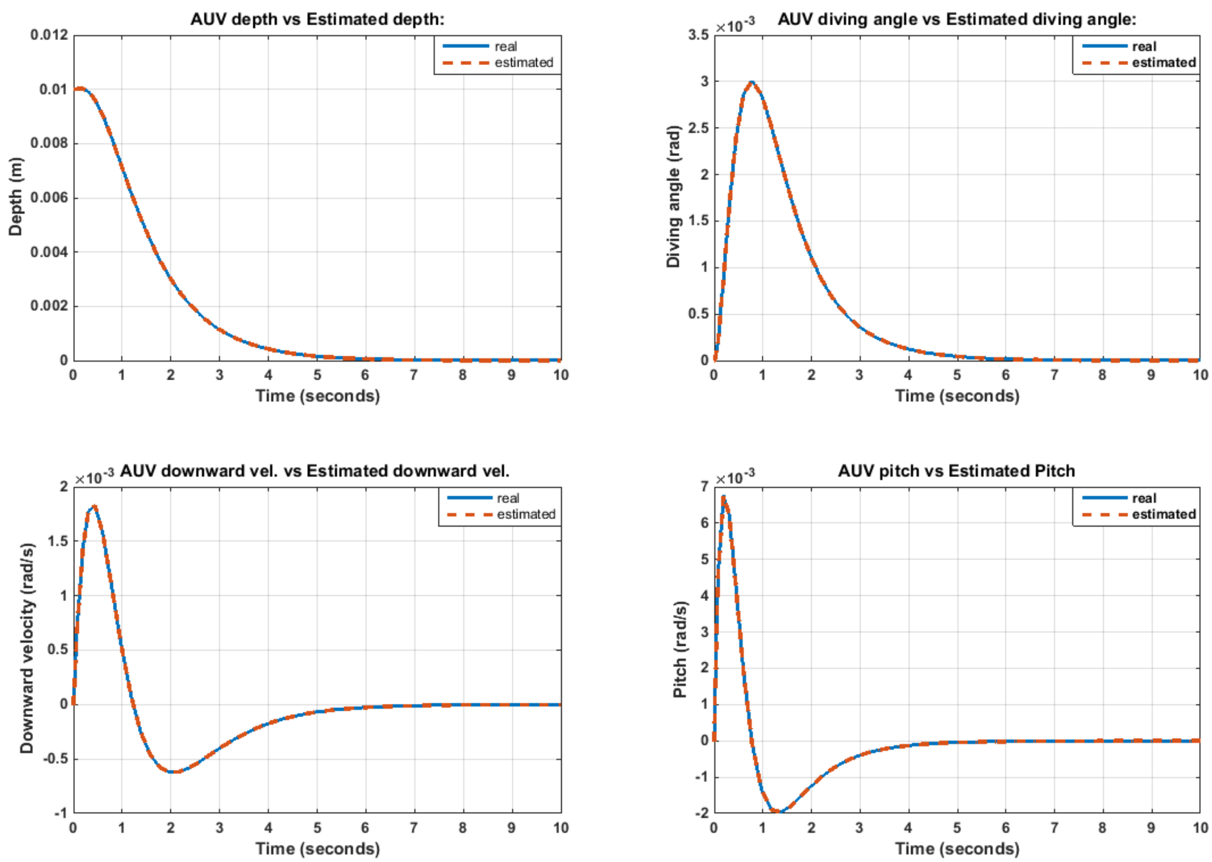

Figure 3.4 Comparative plots of system and estimated states under state-feedback control

The above plots show that the observer designed for the state-feedback controller is estimating the states perfectly.

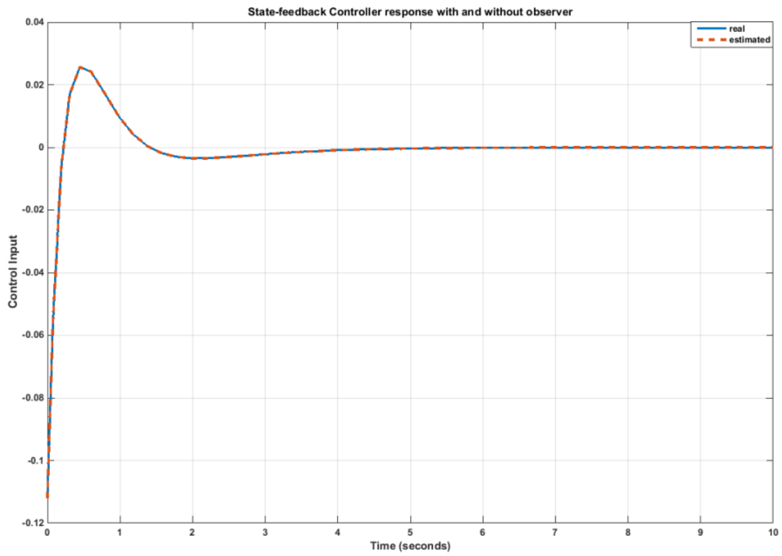

Figure 3.5 Comparison of state-feedback control input with and without observer

3.7 Stabilization using Linear Optimal Control Design

A nonlinear optimal regulation problem is considered for an input affine continuous nonlinear AUV system having state space representation as described in (3.2).

Linear Optimal control design approach is a control technique based on linearization of a nonlinear dynamical system. Using the linearized system and control matrices, this technique uses the solution of Algebric Ricatti Equation (ARE). The solution of ARE is then used to develop a control law that minimizes a given cost functional of the nonlinear dynamical system. This control method is extensively used to provide asymptotically stability to nonlinear dynamical systems.

The system under consideration have performance index that is quadratic in 'δ_s' but non-quadratic in 'x' as below:

$$J = \frac{1}{2}\int_0^\infty (x^T Q(x)x + \delta_s^T R(x)\delta_s)dt \tag{3.28}$$

Where $Q \geq 0 : \mathbb{R}^n \to \mathbb{R}^{nxn}$ is states weighing matrix for states and

$R > 0 : \mathbb{R}^n \to \mathbb{R}^{mxm}$ is input weighing matrix.

Now problem formulated below is minimization problem associated with the performance index mentioned in (3.28)

$$\min_{u(t)} \frac{1}{2}\int_0^\infty (x^T Q(x)x + \delta_s^T R(x)\delta_s)dt \tag{3.29}$$

subjected to $\dot{x} = f(x) + g(x)\delta_s$ where x_0 is the initial condition of the states. Solving current problem of optimal control is equivalent to HJE associated solution [54].

In linear case, when $f(x) = Ax$, optimal feedback control can be represented as,

$$\delta_s(x) = -F_{opt}(x)x \tag{3.30}$$

here $F_{opt}(x) \in \mathbb{R}^n$ needs to be chosen to minimize cost in (3.29) associated with the nonlinear system, stabilizing the system to origin such that $\lim_{x\to\infty} x(t) = 0$.

The fundamental linear control method is LQR synthesis method. Representing an LQR design the state feedback controller is designed as

$$\delta_s(x) = -R^{-1}(x)B^T(x)P(x)x \tag{3.31}$$

\here, P(x)>0 is algebraic solution of ARE represented as,

$$A^T(x)P(x) + P(x)A(x) - P(x)B(x)R^{-1}(x)B^T(x)P(x) + Q(x) = 0 \tag{3.32}$$

Now the resulting ARE based optimal controlled trajectory becomes the quasilinear closed loop dynamics solution

$$\dot{x}(t) = [A(x) - B(x)R^{-1}(x)B^T(x)P(x)]x(t) \tag{3.33}$$

Provided the gain $F_{opt}(x)$ in (3.30) minimizing (3.28) is

$$F_{opt}(x) = -R^{-1}(x)B^T(x)P(x) \tag{3.34}$$

From (3.2), we have system and input matrix as,

$$A = \begin{bmatrix} 0 & -u & 1 & 0 \\ 0 & 0 & 0 & 1 \\ 0 & 0 & A_{31} & A_{32} \\ 0 & 0 & A_{41} & A_{42} \end{bmatrix}$$

$$B = \begin{bmatrix} 0 \\ 0 \\ B_{31} \\ B_{41} \end{bmatrix}$$

To solve for P(x), Q is chosen as I_{4x4} and R is taken as 1.

After solving Ricatti equation,

$$P = \begin{bmatrix} 2.4 & -5.5 & 0.8 & -1.4 \\ -5.5 & 0.8 & -1 & 6.6 \\ 0.8 & -1 & 9 & 4 \\ -1.4 & 6.6 & 4 & 4.4 \end{bmatrix} \tag{3.35}$$

Solving for $F_{opt,}$

$$F_{opt} = [1 \quad -4.8 \quad -3.7 \quad -3.6] \tag{3.36}$$

The linear optimal control input for diving nonlinear model of AUV is,

$$\delta_s(x) = -x_1 + 4.8x_2 + 3.8x_3 + 3.6x_4 \tag{3.37}$$

3.7.1 Simulations on MATLAB/Simulink of Linear Optimal Control

The linear optimal control input of (3.37) is then applied on the nonlinear dynamical model of the AUV system on Simulink. The systems state response on the application of linear state feedback control is shown in Figure 3.6 below.

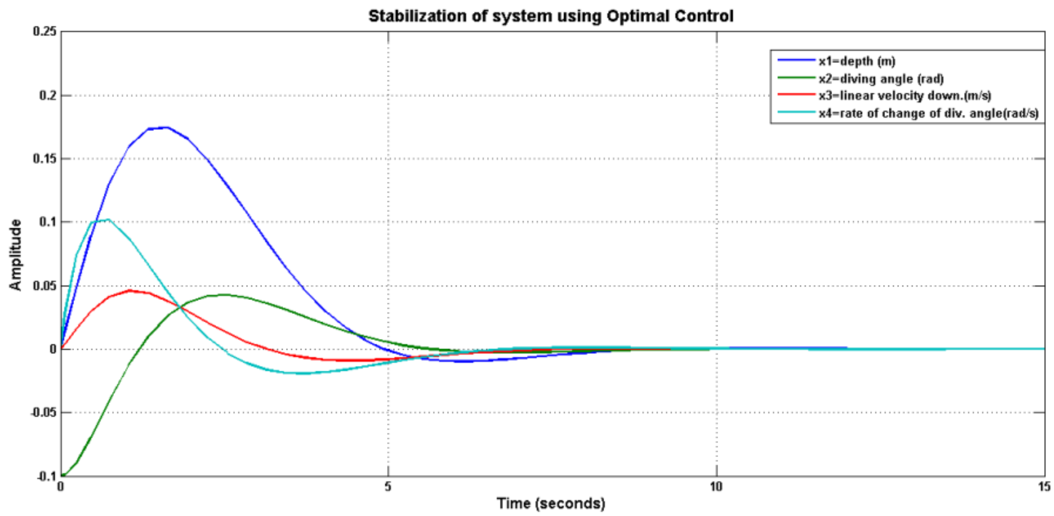

Figure 3.6 : System response on application of linear optimal control

All of the systems states are going to stabilize at origin on the application of linear optimal control in 10 seconds. It is observed that there is 0% steady state error in all states and 17% overshoot in depth during transient response of the system. These results are more promising than that of the linear state-feedback controller. The main aim of the stabilization via optimal control of nonlinear dynamical system is achieved.

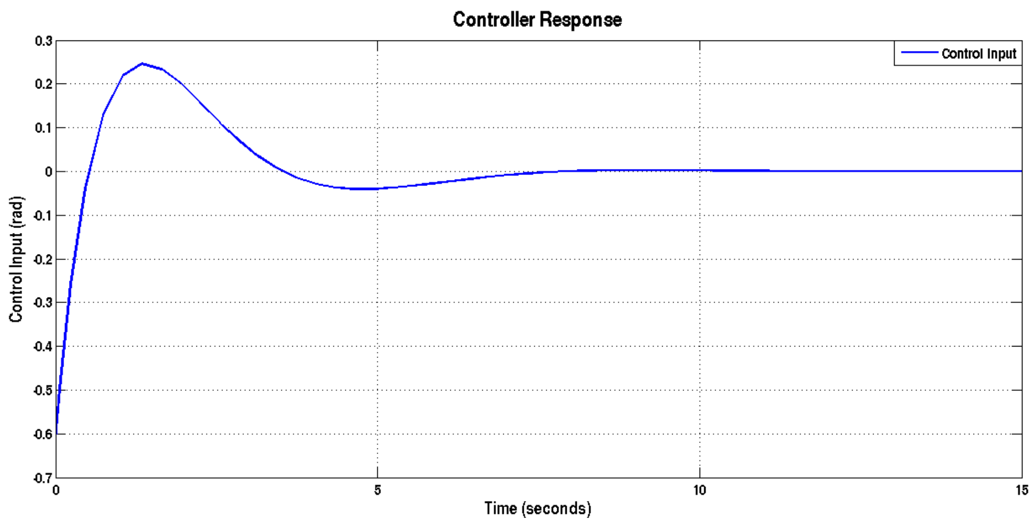

Figure 3.7 : Linear optimal controller response

The linear optimal control input uses very small amount of effort to stabilize the nonlinear dynamical system. Although it has taken more time (10 seconds) than that of the linear state-feedback control input (7 seconds).

Since our basic aim for the linear optimal controller was reliable and cost efficient control, it has achieved its requirements.

3.8 Stabilization using Linear Optimal Control Design with Observer

The poles for the observer are placed at the open left half plane. The gain matrix K found to be

$$K = \begin{bmatrix} 10.1 & -24.3 & -13.7 & -30.7 \end{bmatrix}$$

Simulating the system with the feedback controller and observer, fig.(3.8) shows the effective state estimation of all the system states only using the output of the system.

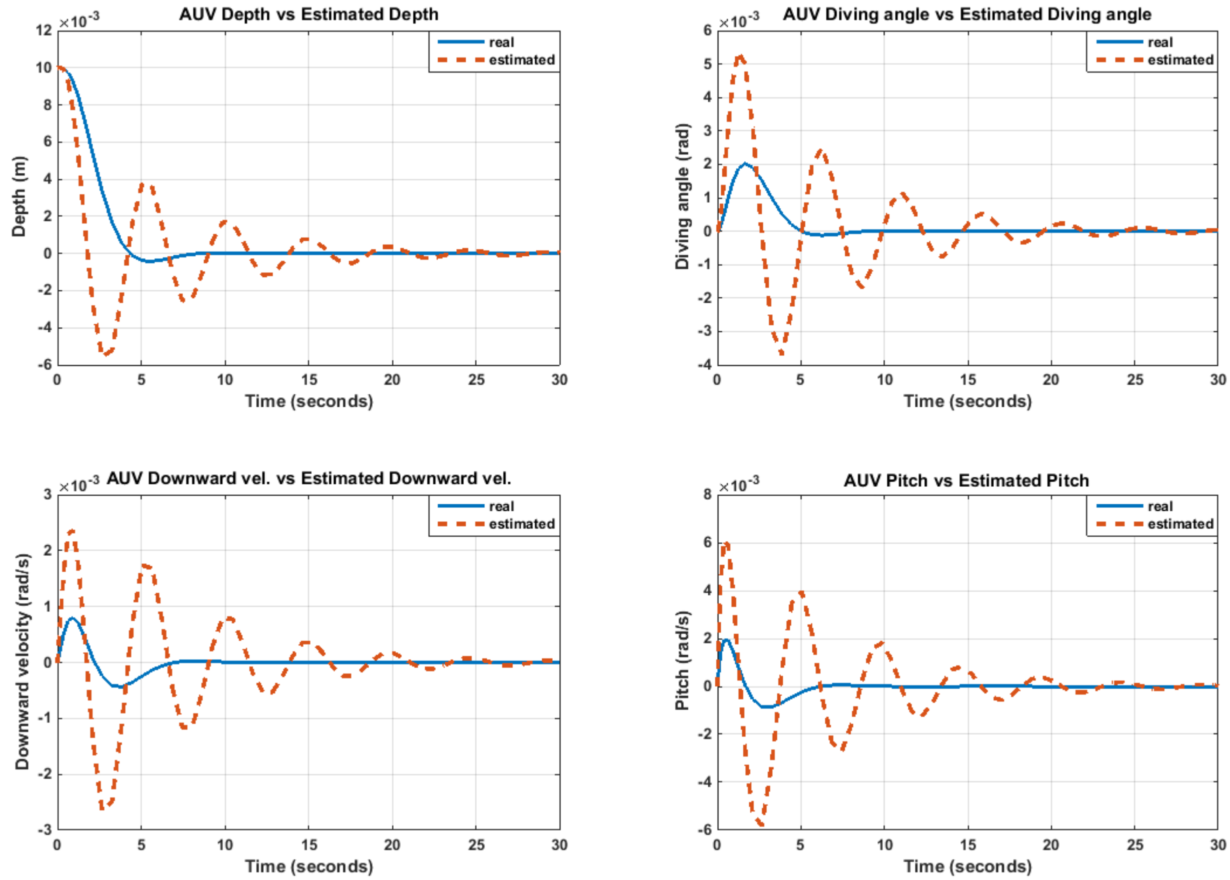

Figure 3.8 Comparative plots of system and estimated states under optimal control

The above plots show that the observer designed for the optimal state-feedback controller is estimating the states.

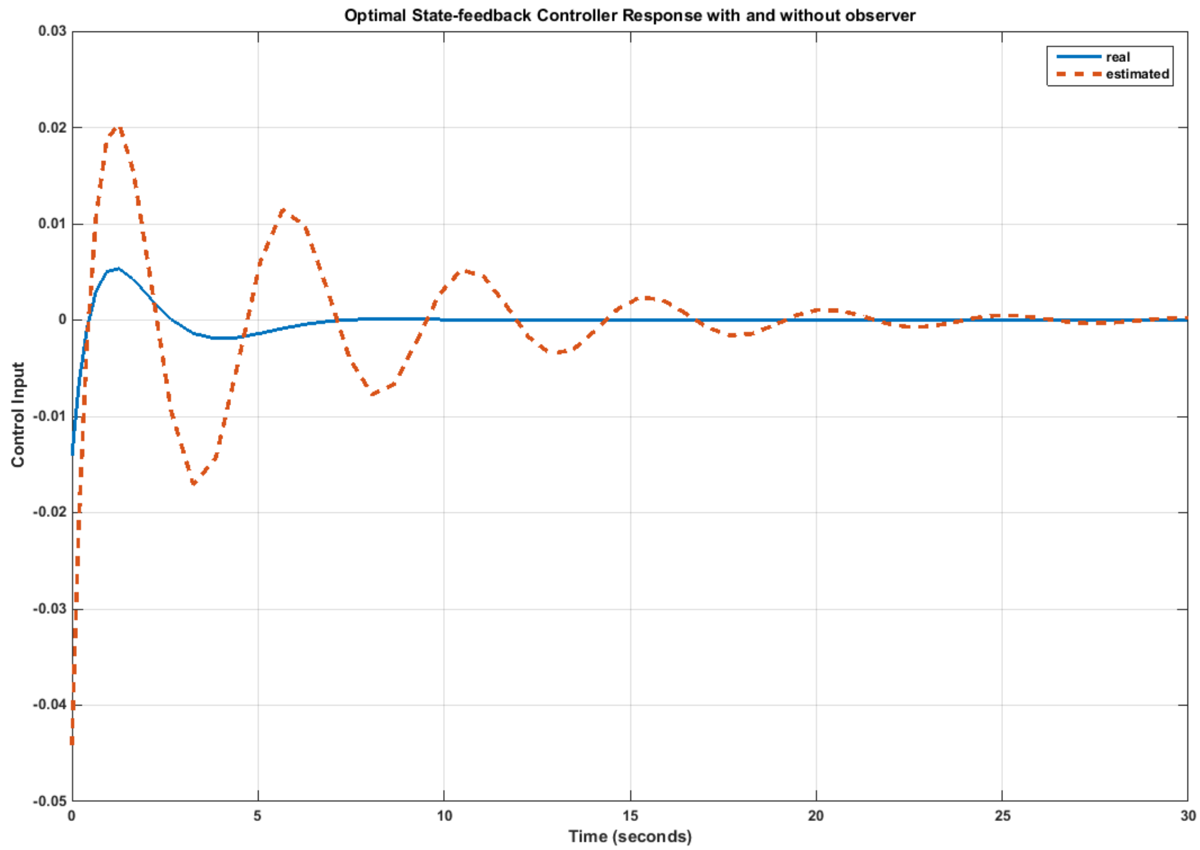

Figure 3.9 Comparison of optimal control input with and without observer

Fig.(3.9) shows the comparison of controller input with and without observer. It can be seen that there is a little estimation error in controller input.

3.9 Combined Comparison of both controllers:

i) Depth stabilization

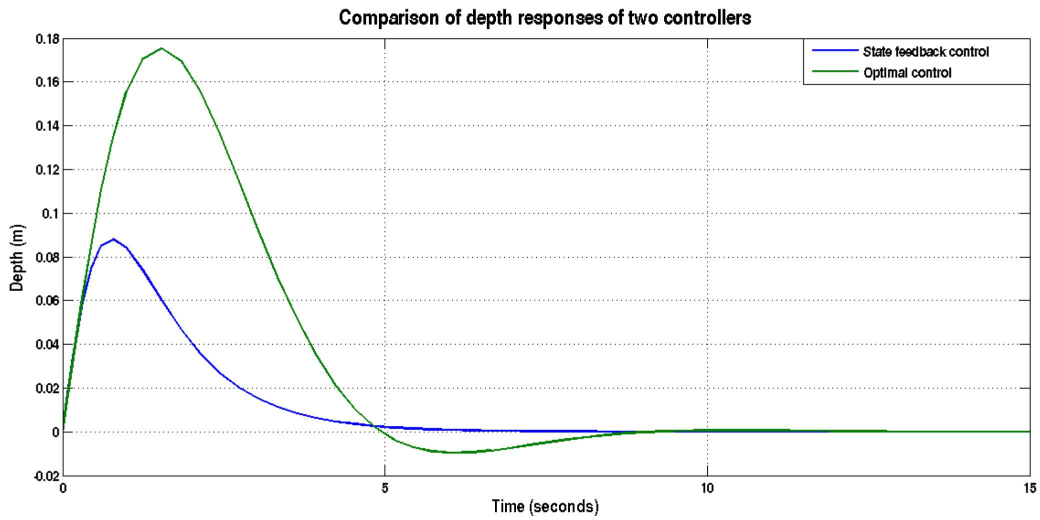

Figure 3.10 Comparison of depth responses of two controllers

It is observed in fig.(3.10) that Optimal control has an overshoot of 18% in transient response of depth state. The optimal control stabilizes the system in 9 seconds whereas the state-feedback controller stabilizes the system in 7 seconds.

ii) Controller input response

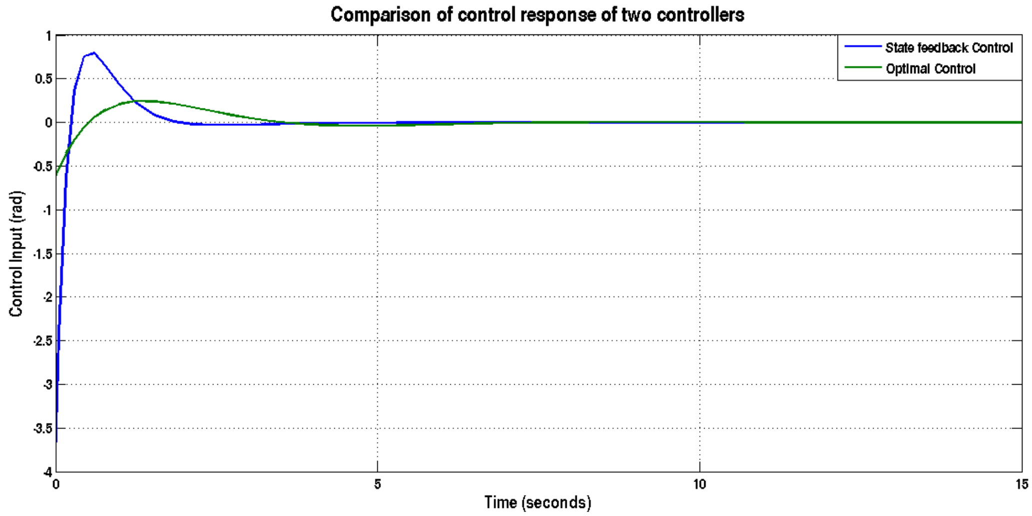

Figure 3.11 Comparison of controller responses of two controllers

The optimal controller has consumed less control effort (that is 0.5) than that of the state-feedback controller (that is 3.5). So it is concluded that the optimal controller is cost effective than state-feedback controller in stabilizing the depth of AUV.

3.10 Estimate of Region of Attraction

In order to estimate the region of attraction of the origin, lyapunov method is taken into account. Let

$$V(x) = x^T P x \tag{3.38}$$

to be a lyapunov function candidate for given system.

It is supposed that about origin, a unit circle is a domain D satisfying, $\dot{V}(x) < 0, \forall\ 0 < \|x\| < r$ and a constant term $a > 0$ such that $\Omega_a = V(x) \le a\ \ , \Omega_a \subset D$.

$$\text{Take } a = \min_{\|x\|=r} x^T P x = \lambda_{\min}(P) r^2 \tag{3.39}$$

$$\{x^T P x < a\} \subset \{\|x\| < r\} \tag{3.40}$$

All of the trajectories starting in the set $\{x^T P x < a\}$ approached he origin as t tends to ∞. Hence, $\{x^T P x < a\}$ is the subset (estimate) of the region of attraction.

Calculating the eigenvalues of P from (3.35),

$$\begin{aligned} \lambda_1 &= 0.18 \\ \lambda_2 &= 0.84 \\ \lambda_3 &= 11 \\ \lambda_4 &= 24.6 \end{aligned} \tag{3.41}$$

The minimum valued eigenvalue of P is $\lambda_{\min}(P) = 0.18$.

Here $\|x\| < r$ is taken 1.

Now, $a = \min_{\|x\|=r} x^T P x = \lambda_{\min}(P) r^2 = 0.18 * (1)$

a=0.18

$\Omega_a = \{V(x) \le 0.18\}$ is the region of attraction of the system is a domain D.

Chapter 4

NON-LINEAR CONTROL DESIGNS FOR AUV

4.1 Introduction

This chapter details about developing non-linear control designs for non-linear AUV dynamical AUV system. The nonlinear dynamical equations of motion of AUV in diving plane are first feedback linearized. The corresponding normal form of the nonlinear dynamical system is then derived. Then nominal control is implemented for stabilization of the depth of AUV with state feedback controller. SMC is then established and is implemented with the nominal stabilizing control. Optimal controller is then designed and implemented with the nominal stabilizing control. Then a combination of Optimal controller + SMC is designed and a comparison of feedback controller and Optimal controller is carried out. Furthermore to cater the model or input uncertainty Lyapunov Redesign controller is used with the nominal controller. A comparison of Lyapunov Redesign controller and the Optimal controller + SMC is carried out. At last, the Inverse optimal controller for the system is designed.

Detailed stability analysis of SMC, Lyapunov Redesign and Inverse Optimal Controllers are also included in this chapter.

4.2 Feedback Linearization

A nonlinear control system admitting normal form of controller is said to be feedback linearizable, if changing of coordinates transforms it to linear system.

AUV system in diving plane is a SISO system of the form:

$$\dot{x} = f(x) + g(x)\delta_s \tag{4.1}$$

$$y = h(x) \tag{4.2}$$

here g(x), h(x) and f(x) are sufficiently smooth in a domain $D \subset \Re^n$.

The state equations of the system under consideration are:

$$\begin{aligned}
\dot{x}_1 &= x_3 \cos x_2 - u \sin x_2 \\
\dot{x}_2 &= x_4 \\
\dot{x}_3 &= A_{31}x_3 + A_{32}x_4 + B_{31}\delta_s \\
\dot{x}_4 &= A_{41}x_3 + A_{42}x_4 + B_{41}\delta_s
\end{aligned} \tag{4.3}$$

And the output is

$$y = x_1 \tag{4.4}$$

The capability that transforms a dynamical nonlinear system equations described in (4.3) to controllable linear system using feedback approach and cancelling nonlinear terms needs dynamical nonlinear system having structure form of

$$\dot{x} = Ax + Bo(x)[u - \chi(x)] \tag{4.5}$$

here $A \in \Re^{nxn}$, $B \in \Re^{nxp}$ with (A,B) as controllable pair.

The functions $\chi : \Re^n \to \Re^p \; and \; o : \Re^n \to \Re^{pxp}$ are defined in a domain $D \subset R^n$ containing origin. The matrix $o(x)$ is non-singular $\forall x \subset D$. If the state equation of the form (4.3) takes the form of (4.5), then the nonlinear state equations using state-feedback may be linearize in the form

$$u = \chi(x) + \beta(x)v \tag{4.6}$$

here

$$\beta(x) = o^{-1}(x) \tag{4.7}$$

Now the nonlinear state equation (4.5) becomes,

$$\dot{x} = Ax + Bv \tag{4.8}$$

The new control variable ‘v’ can be implemented on the system to stabilize it.

It is easy to analyze that the nonlinear state equations of the diving model of AUV presented in (4.3) is not in the feedback linearization form as in (4.6).

The basic aim of feedback linearization is to reduce a nonlinear dynamical, typical system into a controllable linear system. The linear controllable form achieved is called normal form of nonlinear dynamical system.

4.2.1 Normal Form Transformation

First of all the relative degree 'ρ' of the system is required to be finding out. For this purpose the output of the system is differentiated number of times until the control input u shows up.

Since in this case,

$$y = x_1$$

$$\dot{y} = \dot{x}_1 = x_3 \cos x_2 - u \sin x_2$$

$$\ddot{y} = -x_3 \sin x_2 \dot{x}_2 - u \cos x_2 \dot{x}_2 + \dot{x}_3 \cos x_2$$

$$\ddot{y} = -x_3 x_4 \sin x_2 - u x_4 \cos x_2 + A_{31} x_3 \cos x_2 + A_{32} x_4 \cos x_2 + B_{31} \cos x_2 \delta_s$$

Since the control term δ_s appears in the second derivative of the output, the system has relative degree $\rho = 2 \; in \; R^4$.

Theorem 4.1

Consider the system (4.1)-(4.2), and suppose it has relative degree $\rho < n$ *, then for every* $x_0 \in D$ *, a N neighbourhood of* x_0 *with functions* $\phi_1(x), \ldots, \phi_{n-p}(x)$ *that are smooth, exists such that*

$$\frac{\partial \phi_j}{\partial x} g(x) = 0, \quad for\, 1 \le j \le n-p, \forall\, x \in D_0$$

(4.8)

is fulfilled $\forall x \in N$ *with following mapping*

$$T(x) = \begin{bmatrix} \phi_1(x) \\ \vdots \\ \phi_{n-\rho}(x) \\ \text{---------} \\ h(x) \\ \vdots \\ L_f^{\rho-1} h(x) \end{bmatrix} = \begin{bmatrix} \eta \\ \text{---} \\ \xi \end{bmatrix} \tag{4.9}$$

restricted to N, is a diffeomorphism on N, here ϕ_1 *to* $\phi_{n-\rho}$ *needs to be selected so T(x) becomes diffeomorphism within* $D_0 \subset D$ *.*

As per theorem 4.1, the diffeomorphism of the system in (4.3) will become of the form,

$$T(x) = \begin{bmatrix} \eta \\ \text{---} \\ \xi \end{bmatrix} = \begin{bmatrix} \phi_1(x) \\ \phi_2(x) \\ \text{---------} \\ h(x) \\ L_f h(x) \end{bmatrix} \tag{4.10}$$

While to choose $\phi_1(x)$ and $\phi_2(x)$, the condition in (4.8) must be satisfied.

$$g = [0 \quad 0 \quad B_{31} \quad B_{41}]^T$$

Choosing $\phi_1(x) = x_2$ leads to $\frac{\partial \phi_1(x)}{\partial x} = [0 \quad 1 \quad 0 \quad 0]$ satisfies $\frac{\partial \phi_1(x)}{\partial x}.g = 0$

Now choosing $\phi_2(x) = \frac{x_3}{B_{31}} - \frac{x_4}{B_{41}}$ leads to $\frac{\partial \phi_2(x)}{\partial x} = \begin{bmatrix} 0 & 0 & \frac{1}{B_{31}} & -\frac{1}{B_{41}} \end{bmatrix}$ satisfies $\frac{\partial \phi_2(x)}{\partial x}.g = 0$

Now (4.10) becomes,

$$T(x) = \begin{bmatrix} x_2 \\ \frac{x_3}{B_{31}} - \frac{x_4}{B_{41}} \\ \hline x_1 \\ x_3 \cos x_2 - u \sin x_2 \end{bmatrix} \tag{4.11}$$

where,

$$\begin{aligned} \eta_1 &= x_2 \\ \eta_2 &= \frac{x_3}{B_{31}} - \frac{x_4}{B_{41}} \\ \xi_1 &= x_1 \\ \xi_2 &= x_3 \cos x_2 - u \sin x_2 \end{aligned} \tag{4.12}$$

Writing x_1, x_2, x_3 and x_4 in terms of η_1, η_2, ξ_1 and ξ_2,

$$x_1 = \xi_1$$

(4.13)

$$x_2 = \eta_1 \tag{4.14}$$

For x_3 ,

$$\xi_2 = x_3 \cos x_2 - u \sin x_2$$

$$x_3 = \frac{1}{\cos \eta_1} \xi_2 + u \frac{\sin x_2}{\cos x_2}$$

$$x_3 = \xi_2 \sec \eta_1 + u \tan \eta_1 \tag{4.15}$$

For x_4 , from (4.12)

$$\eta_2 = \frac{x_3}{B_{31}} - \frac{x_4}{B_{41}}$$

Placing x_3 produces, $\eta_2 = \frac{1}{B_{31}} \xi_2 \sec \eta_1 - \frac{1}{B_{41}} u \sin \eta_1 - \frac{x_4}{B_{41}}$

$$\frac{x_4}{B_{41}} = -\eta_2 + \frac{1}{B_{31}} \xi_2 \sec \eta_1 + \frac{1}{B_{31}} u \tan \eta_1$$

$$x_4 = -B_{41}\eta_2 + \frac{B_{41}}{B_{31}} \xi_2 \sec \eta_1 + \frac{B_{41}}{B_{31}} u \tan \eta_1 \tag{4.16}$$

Now substituting the values of $x_1, x_2, x_3 \; and \; x_4$ in system equations (4.3) to get the normal form of the system,

$$\dot{\eta}_1 = \dot{x}_2 = x_4$$

$$\dot{\eta}_1 = \frac{B_{41}}{B_{31}}\xi_2 \sec\eta_1 + \frac{B_{41}}{B_{31}} u \tan\eta_1 - B_{41}\eta_2 \tag{4.17}$$

$$\dot{\eta}_2 = \frac{\dot{x}_3}{B_{31}} - \frac{\dot{x}_4}{B_{41}}$$

$$\dot{\eta}_2 = \frac{A_{31}}{B_{31}} x_3 + \frac{A_{32}}{B_{31}} x_4 + \frac{\cancel{B_{31}}}{\cancel{B_{31}}} \cancel{\delta}_s - \frac{A_{41}}{B_{41}} x_3 - \frac{A_{42}}{B_{42}} x_4 - \frac{\cancel{B_{41}}}{\cancel{B_{41}}} \cancel{\delta}_s$$

$$\dot{\eta}_2 = \left(\frac{A_{31}}{B_{31}} - \frac{A_{41}}{B_{41}} \right) x_3 + \left(\frac{A_{32}}{B_{31}} - \frac{A_{42}}{B_{41}} \right) x_4$$

$$\dot{\eta}_2 = \left(\frac{A_{31}}{B_{31}} - \frac{A_{41}}{B_{41}} \right)\left(\xi_2 \sec\eta_1 + u \tan\eta_1 \right) + \left(\frac{A_{32}}{B_{31}} - \frac{A_{42}}{B_{41}} \right)\left(-B_{41}\eta_2 + \frac{B_{41}}{B_{31}}\xi_2 \sec\eta_1 + \frac{B_{41}}{B_{31}} u \tan\eta_1 \right)$$

$$\dot{\eta}_2 = \left(\frac{A_{31}}{B_{31}} - \frac{A_{41}}{B_{41}} \right)\xi_2 \sec\eta_1 + \left(\frac{A_{31}}{B_{31}} - \frac{A_{41}}{B_{41}} \right) u \tan\eta_1 - \left(\frac{A_{32} B_{41}}{B_{31}} - \frac{A_{42} \cancel{B_{41}}}{\cancel{B_{41}}} \right)\eta_2$$
$$+ \left(\frac{A_{32} B_{41}}{B^2_{31}} - \frac{A_{42} \cancel{B_{41}}}{\cancel{B_{41}} B_{31}} \right)\xi_2 \sec\eta_1 + \left(\frac{A_{32} B_{41}}{B^2_{31}} - \frac{A_{42} \cancel{B_{41}}}{\cancel{B_{41}} B_{31}} \right) u \tan\eta_1$$

$$\dot{\eta}_2 = \left(\frac{A_{31}}{B_{31}} - \frac{A_{41}}{B_{41}} + \frac{A_{32} B_{41}}{B^2_{31}} - \frac{A_{42}}{B_{31}} \right)\xi_2 \sec\eta_1 + \left(\frac{A_{31}}{B_{31}} - \frac{A_{41}}{B_{41}} + \frac{A_{32} B_{41}}{B^2_{31}} - \frac{A_{42}}{B_{31}} \right) u \tan\eta_1 - \left(\frac{A_{32} B_{41}}{B_{31}} - A_{42} \right)\eta_2$$

(4.18)

$$\dot{\xi}_1 = \xi_2$$

(4.19)

$$\dot{\xi}_2 = -x_3 \sin x_2 \dot{x}_2 + \cos x_2 \dot{x}_3 - u \cos x_2 \dot{x}_2$$

$$\dot{\xi}_2 = -x_3 \sin \eta_1 \dot{\eta}_1 + \cos \eta_1 \dot{x}_3 - u \cos \eta_1 \dot{\eta}_1$$

$$\dot{\xi}_2 = (-\xi_2 \tan \eta_1 - u \sin \eta_1 \tan \eta_1)\dot{\eta}_1 + A_{31} x_3 \cos \eta_1 + A_{32} x_4 \cos \eta_1 + B_{31} \cos \eta_1 \delta_s - u\dot{\eta}_1 \cos \eta_1$$

Since, $\dot{\eta}_1 = \frac{B_{41}}{B_{31}} \xi_2 \sec \eta_1 + \frac{B_{41}}{B_{31}} u \tan \eta_1 - B_{41} \eta_2$

And $x_3 = \xi_2 \sec \eta_1 + u \tan \eta_1$

$$\begin{aligned}\dot{\xi}_2 = {} & B_{41}\eta_2\xi_2 \tan \eta_1 + B_{41} u \eta_2 \sin \eta_1 \tan \eta_1 - \frac{B_{41}}{B_{31}} \xi_2^2 \tan \eta_1 \sec \eta_1 - \frac{B_{41}}{B_{31}} u \xi_2 \tan^2 \eta_1 - \frac{B_{41}}{B_{31}} u \xi_2 \tan^2 \eta_1 \\ & - \frac{B_{41}}{B_{31}} u^2 \sin \eta_1 \tan^2 \eta_1 + A_{31}\xi_2 + A_{31} u \sin \eta_1 - A_{32} B_{41} \eta_2 \cos \eta_1 + \frac{A_{32} B_{41}}{B_{31}} \xi_2 + \frac{A_{32} B_{41}}{B_{31}} u \sin \eta_1 \\ & + B_{31} \cos \eta_1 \delta_s + B_{41} u \eta_2 \cos \eta_1 - \frac{B_{41}}{B_{31}} u \xi_2 - \frac{B_{41}}{B_{31}} u^2 \sin \eta_1\end{aligned}$$

$$\begin{aligned}\dot{\xi}_2 = {} & \left(A_{31} + \frac{A_{32} B_{41}}{B_{31}} \right) \xi_2 + \left(A_{31} + \frac{A_{32} B_{41}}{B_{31}} - \frac{B_{41}}{B_{31}} u^2 \right) \sin \eta_1 + \left(B_{41} u - A_{32} B_{41} \right) \eta_2 \cos \eta_1 + B_{41} u \eta_2 \sin \eta_1 \tan \eta_1 \\ & - \frac{B_{41}}{B_{31}} u^2 \sin \eta_1 \tan^2 \eta_1 - 2 \frac{B_{41}}{B_{31}} u \xi_2 \tan^2 \eta_1 + B_{41} \eta_2 \xi_2 \tan \eta_1 - \frac{B_{41}}{B_{31}} \xi_2^2 \tan \eta_1 \sec \eta_1 + B_{31} \cos \eta_1 \delta_s\end{aligned} \tag{4.20}$$

Now the normal form of the nonlinear dynamical system of (4.3) can be represented by the following set of equations:

$$
\begin{aligned}
\dot{\eta}_1 &= \frac{B_{41}}{B_{31}}\xi_2 \sec\eta_1 + \frac{B_{41}}{B_{31}}u\tan\eta_1 - B_{41}\eta_2 \\
\dot{\eta}_2 &= \left(\frac{A_{31}}{B_{31}} - \frac{A_{41}}{B_{41}} + \frac{A_{32}B_{41}}{B^2_{31}} - \frac{A_{42}}{B_{31}}\right)\xi_2 \sec\eta_1 + \left(\frac{A_{31}}{B_{31}} - \frac{A_{41}}{B_{41}} + \frac{A_{32}B_{41}}{B^2_{31}} - \frac{A_{42}}{B_{31}}\right)u\tan\eta_1 - \left(\frac{A_{32}B_{41}}{B_{31}} - A_{42}\right)\eta_2 \\
\dot{\xi}_1 &= \xi_2 \\
\dot{\xi}_2 &= \left(A_{31} + \frac{A_{32}B_{41}}{B_{31}}\right)\xi_2 + \left(A_{31} + \frac{A_{32}B_{41}}{B_{31}} - \frac{B_{41}}{B_{31}}u^2\right)\sin\eta_1 + \left(B_{41}u - A_{32}B_{41}\right)\eta_2\cos\eta_1 + B_{41}u\eta_2\sin\eta_1\tan\eta_1 \\
&\quad - \frac{B_{41}}{B_{31}}u^2\sin\eta_1\tan^2\eta_1 - 2\frac{B_{41}}{B_{31}}u\xi_2\tan^2\eta_1 + B_{41}\eta_2\xi_2\tan\eta_1 - \frac{B_{41}}{B_{31}}\xi_2^2\tan\eta_1\sec\eta_1 + B_{31}\cos\eta_1\delta_s
\end{aligned}
\tag{4.21}
$$

The above set of equations can be simplified in the form

$$
\begin{aligned}
\dot{\eta}_1 &= C_1\xi_2\sec\eta_1 + C_2\tan\eta_1 - C_3\eta_2 \\
\dot{\eta}_2 &= C_4\xi_2\sec\eta_1 + C_5 u\tan\eta_1 - C_6\eta_2 \\
\dot{\xi}_1 &= \xi_2 \\
\dot{\xi}_2 &= C_7\xi_2 + C_8\sin\eta_1 + C_9\eta_2\cos\eta_1 + C_{10}\eta_2\sin\eta_1\tan\eta_1 - C_{11}\sin\eta_1\tan^2\eta_1 \\
&\quad - C_{12}\xi_2\tan^2\eta_1 + C_{13}\eta_2\xi_2\tan\eta_1 - C_{14}\xi_2^2\tan\eta_1\sec\eta_1 + C_{15}\cos\eta_1\delta_s
\end{aligned}
\tag{4.22}
$$

And the output becomes,

$$
y = \xi_1 \tag{4.23}
$$

Where $C_1, C_2, \cdots, C_{15}$ are the coefficients replaced from (4.21).

4.3 Control Design and Analysis

The normal form of the system divides the system into two parts i.e the first two states of the systems $\eta_1\ and\ \eta_2$ are the internal states of the system and the last two states $\xi_1\ and\ \xi_2$ are the external states of the system. It is clearly seen that in (4.3) the control input $'\delta_s'$ appears in two states where as in the normal form the control input 'δ_s' appears only in one state of the external part. This makes the internal states of the system unobservable from the control input.

Now choosing the control input,

$$\breve{\delta}_s = -\frac{1}{C_{15}\cos\eta_1}(C_7\xi_2 + C_8\sin\eta_1 + C_9\eta_2\cos\eta_1 + C_{10}\eta_2\sin\eta_1\tan\eta_1 - C_{11}\sin\eta_1\tan^2\eta_1$$
$$- C_{12}\xi_2\tan^2\eta_1 + C_{13}\eta_2\xi_2\tan\eta_1 - C_{14}\xi_2^2\tan\eta_1\sec\eta_1) + v \tag{4.24}$$

will reduces the (4.22) to the form

$$\dot{\eta} = f_0(\eta, \xi) \tag{4.25}$$

$$\dot{\xi} = A\xi + Bv \tag{4.26}$$

Equation (4.26) can easily be stabilized by a stabilizing controller $v = -F\xi$, where F needs to be selected to make (A-BF) Hurwitz. The under consideration closed loop system

$$\dot{\eta} = f_0(\eta, \xi) \tag{4.27}$$

$$\dot{\xi} = (A - BF)\xi \tag{4.28}$$

asymptotic stability at origin follows stability of origin of system internal state's $\dot{\eta} = f_0(\eta, 0)$ as shown in lemma 13.1 [55]. It has been verified that internal states of the system have zeron dynamics $\dot{\eta} = f_0(\eta, 0)$ that are BIBO stable in the domain of interest and the normal system form under consideration is minimum phase.

Now the objective of the control design is to design a controller for the external part of the system such that the depth of the AUV system stabilizes.

Important Note:

It is important to mention that $\eta_1 = x_2 = diving\ angle\ of\ AUV$ is present in the controller of (4.29) in the denominator as an argument of cosine function. For diving angle $\eta_1 = x_2 = 90^0$ the controller of (4.29) will fails to stabilize the AUV.

4.3.1 Stabilizing controller

The stabilizing controller for (4.22) is selected as,

$$\delta_s = -\frac{1}{C_{15}\cos\eta_1}(C_7\xi_2 + C_8\sin\eta_1 + C_9\eta_2\cos\eta_1 + C_{10}\eta_2\sin\eta_1\tan\eta_1 - C_{11}\sin\eta_1\tan^2\eta_1 - C_{12}\xi_2\tan^2\eta_1 + C_{13}\eta_2\xi_2\tan\eta_1 - C_{14}\xi_2^2\tan\eta_1\sec\eta_1) - f_1\xi_1 - f_2\xi_2 \tag{4.29}$$

where the gains f_1 and f_2 are selected such that (A-BF) in (4.28) becomes Hurwitz.

- Simulation of Stabilizing Controller

  For simulation, the poles of the external part of the normal form of the AUV system in diving plane are selected at LHP. The corresponding gains are $f_1 = 8,\ f_2 = 6$ **.**

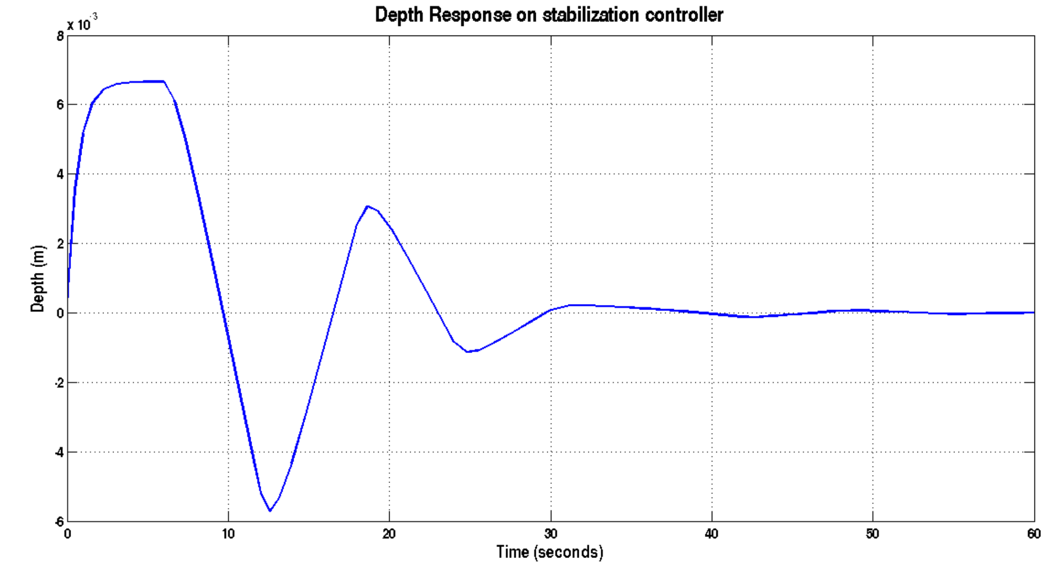

Figure 4.1 Depth response on application of nonlinear stabilization controller

On the application of nonlinear stabilization controller of (4.29), the depth of the AUV stabilizes at 0 m in 35 seconds with maximum overshoot of 0.63%.

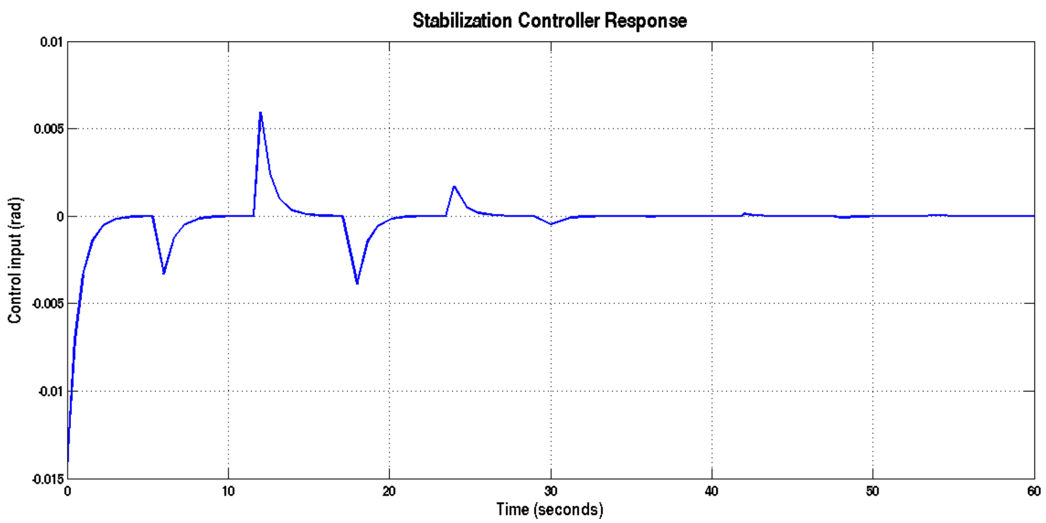

Figure 4.2 Stabilization controller response

The stabilization controller response in fig.4.2 shows that the controller has used more effort during initial transient time to bring the system to stabilization as compared to steady state.

4.3.2 Sliding Mode Controller

SMC is calculated then implemented on the system under consideration. The proposed controller is based on the methodology proposed in [56]. The control objective of the SMC is that the system states X tracks a desired reference X_D.

The error state vector is then can be represented as,

$$\tilde{X} = X - X_D = \begin{bmatrix} x_1 - x_{D1} \\ \vdots \\ x_n - x_{Dn} \end{bmatrix} \tag{4.30}$$

X_D in (4.30) represents vector of desired states.

For SMC designing, the sliding surface is defined as,

$$\sigma = S^T X \tag{4.31}$$

This sliding surface can be written in the error coordinates as,

$$\sigma = S^T \tilde{X} \tag{4.32}$$

$$\sigma = [s_1 \quad \cdots \quad s_n] \begin{bmatrix} x_1 - x_{D1} \\ \vdots \\ x_n - x_{Dn} \end{bmatrix} \tag{4.33}$$

The first step here is to choose the surface coefficients vector S such that $\lim_{t \to \infty} \dot{\sigma} \to 0$ $i.e$ $\lim_{t \to \infty} \sigma \to 0$, that will ensure that $\lim_{t \to \infty} \tilde{X} = \lim_{t \to \infty} (X - X_D) \to 0$.

Now let suppose quadratic lyapunov function of the form,

$$V(\sigma) = \frac{1}{2}\sigma^2 \tag{4.34}$$

To determine the surface coefficients vector S that achieves the above mentioned objective, the conditions needs to be determined that would make $\dot{V}(\sigma)$ negative definitive. Let's suppose,

$$\dot{V}(\sigma) = \sigma\dot{\sigma} \leq -\rho^2 \left|\sigma\right|^2 \tag{4.35}$$

Where $\rho > 0$ is a design parameter.

The condition expressed in (4.35) can be written as,

$$\dot{\sigma} \leq -\rho^2 \,\mathrm{sgn}(\sigma) \tag{4.36}$$

This will ensure that under consideration AUV system's trajectories converge to sliding surface in finite time. Now differentiating sliding surface in (4.33) along the trajectories of the system

$$\dot{\sigma} = S^T \dot{\tilde{X}} \tag{4.37}$$

here $\dot{\tilde{X}} = AX + B\delta_s - \dot{X}_D$. Now the differentiated sliding surface becomes

$$\dot{\sigma} = S^T (AX + B\delta_s - \dot{X}_D) \leq -\rho^2 \,\mathrm{sgn}(\sigma) \tag{4.38}$$

Solving for control input δ_s

$$S^T AX + S^T B\delta_s - S^T \dot{X}_D \le -\rho^2 \operatorname{sgn}(\sigma)$$

$$\delta_s \le \frac{-S^T AX + S^T \dot{X}_D - \rho^2 \operatorname{sgn}(\sigma)}{S^T B}$$

$$\delta_s \le -(S^T B)^{-1} S^T AX + (S^T B)^{-1} S^T \dot{X}_D - (S^T B)^{-1} \rho^2 \operatorname{sgn}(\sigma) \tag{4.39}$$

The above controller equation can be divided into two parts, i.e. the stabilizing controller and the non-linear control.

$$\delta_s = \frown{\delta}_s + \overline{\delta}_s \tag{4.40}$$

Where the stabilizing control is described as

$$\frown{\delta}_s = -(S^T B)^{-1} S^T AX + (S^T B)^{-1} S^T \dot{X}_D \tag{4.41}$$

Whereas the switching controller can be described as

$$\overline{\delta}_s = (S^T B)^{-1} \rho^2 \operatorname{sgn}(\sigma) \tag{4.42}$$

When X_D is constant, the equation (4.41) can be simplified as, $\frown{\delta}_s = -(S^T B)^{-1} S^T AX$

Under stabilizing control

$$\frown{\delta}_s = -FX \tag{4.43}$$

matrix F is selected to place the eigenvalues of the closed loop system at $[\lambda_1 \cdots \lambda_n]$ ensuring the convergence of the closed loop system's trajectories to the sliding surface $i.e \lim_{t \to \infty} \sigma \to 0$, .This results the closed loop system as described below,

$$\dot{X} = AX + B\delta_s$$
$$\dot{X} = (A - BF)X$$

Since $\sigma = S^T \tilde{X} = 0$

And therefore,

$$\dot{\sigma} = S^T \dot{\tilde{X}} = 0$$

Therefore, $\dot{\sigma} = S^T \dot{X} = 0$

$$S^T (A - BF) = 0$$

$$(A - BF)^T S = 0$$

It can be observed that the vector of coefficients of sliding surface S is the eigenvector of $(A - BF)^T$ associated to the null eigenvalue. Now using equations (4.40), (4.42) and (4.43) the AUV system can be written in the error coordinates (4.33) as

$$\dot{\tilde{X}} = (A - BF)\tilde{X} - BFX_D + (S^T B)^{-1} \rho^2 \operatorname{sgn}(\sigma) \tag{4.44}$$

It is obvious that the $sgn(\sigma)$ discontinuous control element causes chattering. Its traditional substitute $sat(\frac{\sigma}{\varepsilon})$ is used in which 'ε' is a small design parameter. The controller of (4.40) becomes,

$$\delta_s = \hat{\delta}_s + \bar{\delta}_s = -F(\tilde{X} + X_D) + (S^T B)^{-1} \rho^2 sat(\frac{\sigma}{\varepsilon}) \tag{4.45}$$

This results the closed loop system as defined

$$\dot{\tilde{X}} = (A - BF)\tilde{X} - BFX_D + (S^T B)^{-1} \rho^2 sat(\frac{\sigma}{\varepsilon}) \tag{4.46}$$

It is concluded that using the SMC of (4.45), trajectories of system in closed loop configuration (4.46) will converges to σ in a given finite time. These trajectories of closed loop system will stay inside the boundary layer defined by $\sigma \leq \varepsilon$ afterwards.

The nonlinear SMC for stabilization of depth is numerically simulated. The nonlinear SMC is thus represented as,

$$\begin{aligned}\bar{\delta}_s = -\frac{1}{C_{15}\cos\eta_1}(C_7\xi_2 + C_8\sin\eta_1 + C_9\eta_2\cos\eta_1 + C_{10}\eta_2\sin\eta_1\tan\eta_1 - C_{11}\sin\eta_1\tan^2\eta_1 \\ - C_{12}\xi_2\tan^2\eta_1 + C_{13}\eta_2\xi_2\tan\eta_1 - C_{14}\xi_2^2\tan\eta_1\sec\eta_1) + (S^T B)^{-1}\rho^2 sat(\frac{\sigma}{\varepsilon})\end{aligned} \tag{4.47}$$

In (4.47), $(S^T B)^{-1} = -1$ and the design parameters $\rho^2 = 1$ *and* $\varepsilon = 0.5$. Now the nonlinear SMC becomes,

$$\bar{\delta}_s = -\frac{1}{C_{15}\cos\eta_1}(C_7\xi_2 + C_8\sin\eta_1 + C_9\eta_2\cos\eta_1 + C_{10}\eta_2\sin\eta_1\tan\eta_1 - C_{11}\sin\eta_1\tan^2\eta_1$$
$$- C_{12}\xi_2\tan^2\eta_1 + C_{13}\eta_2\xi_2\tan\eta_1 - C_{14}\xi_2^2\tan\eta_1\sec\eta_1) - sat(\frac{\sigma}{0.5}) \qquad (4.48)$$

The desired trajectory is set to 0.

4.3.3 SMC with Feedback controller

This technique incorporates the sliding mode controller with feedback controller in series with the nominal nonlinear controller.

The corresponding combined controller becomes,

$$\delta_s + \bar{\delta}_s = -\frac{1}{C_{15}\cos\eta_1}(C_7\xi_2 + C_8\sin\eta_1 + C_9\eta_2\cos\eta_1 + C_{10}\eta_2\sin\eta_1\tan\eta_1 - C_{11}\sin\eta_1\tan^2\eta_1$$
$$- C_{12}\xi_2\tan^2\eta_1 + C_{13}\eta_2\xi_2\tan\eta_1 - C_{14}\xi_2^2\tan\eta_1\sec\eta_1) - f_1\xi_1 - f_2\xi_2 - sat(\frac{\sigma}{0.5}) \qquad (4.49)$$

where $\sigma = 0.5\xi_1 + 1.5\xi_2$

4.3.4 Optimal Controller

Optimal controller is designed for the external part of the AUV system normal form defined in (4.26). The technique used is the same as used in section 3.6 using Algebric Ricatti Equation solution and minimizing the cost of (3.22). The matrix Q is selected as,

$$Q = 0.1I$$

The gain of the optimal controller is found to be $F_{opt_1} = 0.31 \; and \; F_{opt2} = 0.85$. The nonlinear optimal controller for the system in (4.22) becomes,

$$\delta_{s_{opt}} = -\frac{1}{C_{15}\cos\eta_1}(C_7\xi_2 + C_8\sin\eta_1 + C_9\eta_2\cos\eta_1 + C_{10}\eta_2\sin\eta_1\tan\eta_1 - C_{11}\sin\eta_1\tan^2\eta_1 \\ - C_{12}\xi_2\tan^2\eta_1 + C_{13}\eta_2\xi_2\tan\eta_1 - C_{14}\xi_2^2\tan\eta_1\sec\eta_1) - F_{opt_1}\xi_1 - F_{opt_2}\xi_2 \quad (4.50)$$

4.3.5 Optimal Controller with SMC

This technique is used to minimize the control effort of the controller with the robust stabilization qualities of SMC.

The optimal controller with SMC used for depth stabilization has the form,

$$\delta_{s_{opt}} + \overline{\delta}_s = -\frac{1}{C_{15}\cos\eta_1}(C_7\xi_2 + C_8\sin\eta_1 + C_9\eta_2\cos\eta_1 + C_{10}\eta_2\sin\eta_1\tan\eta_1 - C_{11}\sin\eta_1\tan^2\eta_1 \\ - C_{12}\xi_2\tan^2\eta_1 + C_{13}\eta_2\xi_2\tan\eta_1 - C_{14}\xi_2^2\tan\eta_1\sec\eta_1) - F_{opt_1}\xi_1 - F_{opt_2}\xi_2 - sat(\frac{\sigma}{0.5}) \quad (4.51)$$

4.4 Simulation

The combined simulation of the feedback stabilization controller, SMC, feedback with SMC, Optimal and Optimal with SMC as described in equations (4.29), (4.48). (4.49), (4.50) and (4.51) respectively is performed. The parameters used for AUV are described in Appendix-A.

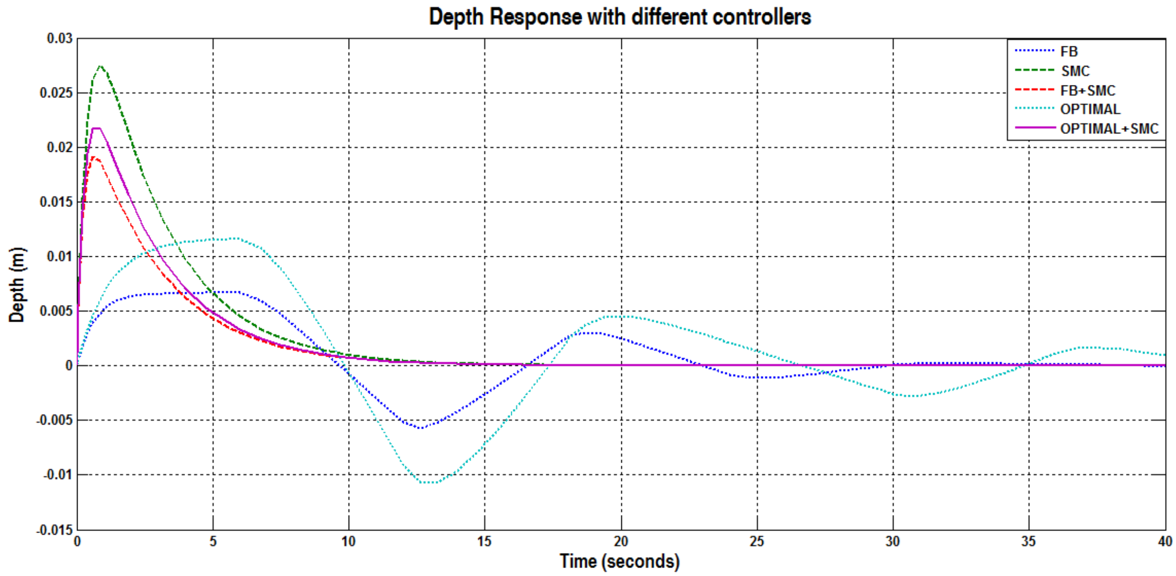

Figure 4.3 Depth response of AUV with different controllers

It can be seen clearly that all of the controllers have stabilized the depth of AUV at 0 meters. The Feedback and optimal controllers alone are stabilizing the system slowly in 40 seconds with less overshoot (1%) in transient time. SMC alone has the highest overshoot of 2.8% at 1.25 seconds. The combined feedback and SMC controller has the maximum overshoot of 1.9% while the combined optimal and SMC controller has the maximum overshoot of 2.1%. All of the three later controllers having SMC are stabilizing faster within 15 seconds.

The two controllers feedback with SMC and optimal with SMC are so close to each other with respect to depth stabilization traits.

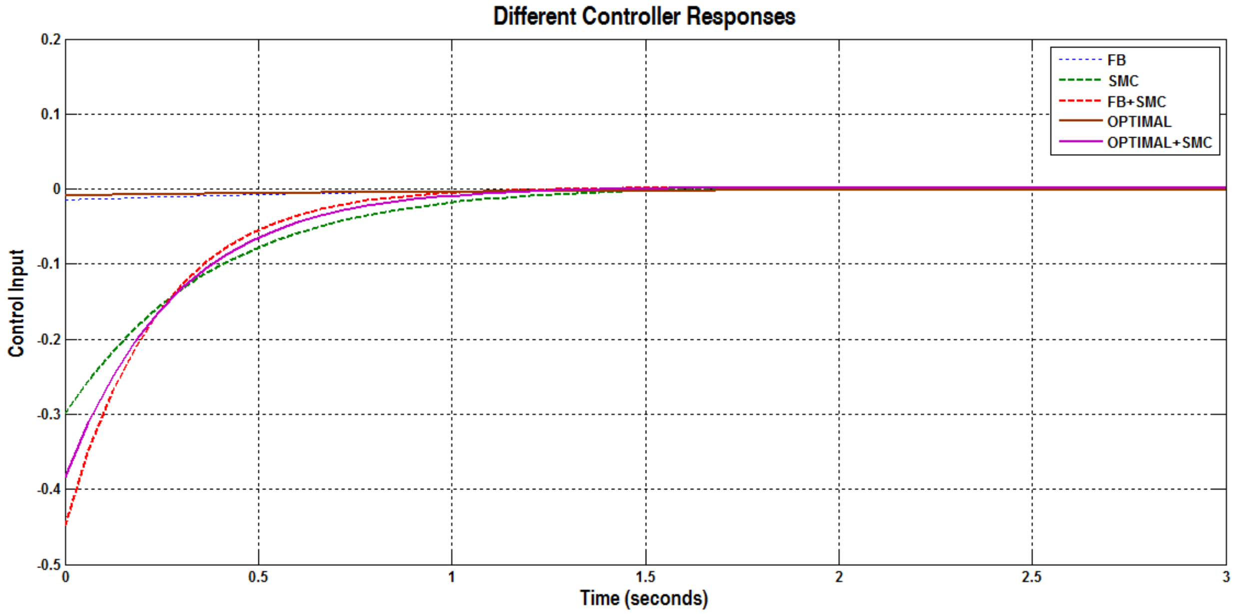

Figure 4.4 Different Controllers Responses

It is observed from the fig.4.4 that the optimal controller alone has used the minimum controller effort to stabilize the system whereas the feedback stabilization controller is at second position after optimal controller. SMC has used an effort input control of 0.3 but is approaching stabilization a little late than that of the combined controllers.

Here the combined controller of feedback and SMC is using more effort than that of the optimal with SMC; therefore the best of the five controllers is the combined control of optimal control and SMC.

4.5 Lyapunov Redesign Approach

Let us consider the system of diving model of AUV as

$$\dot{x} = f(t,x) + G(t,x)[u + \delta(t,x,u)] \tag{4.52}$$

here $u \in R^p$ represents controller input and $x \in R^n$ represents the system's state vector. The functions δ , G and F defined for $(t, x, u) \in [0, \infty) \times D \times R^p, here\, D\, is\, subset\, of\, R^n$ containing origin. Functions δ , G and F are assumed as locally Lipschitz in 'u' and 'x' also piecewise continuous in time. Functions G and f considered as precisely known and δ is supposed to be undisclosed function having numerous uncertain terms because of the uncertainty in parameters and simplification of model. It is supposed that δ fulfills matching condition.

A nonlinear system's nominal model is described below

$$\dot{x} = f(t, x) + G(t, x)u \tag{4.53}$$

Suppose a feedback control $\psi(t, x)$ is designed that uniformly asymptotically stabilizes the nominal closed loop system at origin

$$\dot{x} = f(t, x) + G(t, x)\psi(t, x) \tag{4.54}$$

Further supposing that a lyapunov function for (4.54) is known i.e V(t,x) fulfills the following inequalities

$$\alpha_1(\|x\|) \leq V(t, x) \leq \alpha_2(\|x\|) \tag{4.55}$$

$$\frac{\partial V}{\partial t} + \frac{\partial V}{\partial x}[f(t, x) + G(t, x)\psi(t, x)] \leq -\alpha_3(\|x\|) \tag{4.56}$$

$\forall (t, x) \in [0, \infty) \times D, where\, \alpha_1, \alpha_2\, and\, \alpha_3\, are\, class\, \kappa$ functions. Now assuming that with control input $u = \psi(t, x) + v$, δ fulfills following expression

$$\left\|\delta(t,x,\psi(t,x)+v\right\| \le \rho(t,x)+\kappa_0\left\|v\right\|, \quad 0 \le \kappa_0 \le 1 \tag{4.57}$$

here $\rho : [0,\infty)\times D \rightarrow R$ represents continuous function having positive semi-definite values. It is the measure of the size of the uncertainty.

The main aim of the Lyapunov redesign method is to design a $'v'$ implementing the information regarding the functions ρ, V(x) and constant κ_0 such that controller input designed as $u = \psi(t,x)+v$ stabilizes the system of (4.52) in presence of the uncertainty.

Now the system (4.52) with perturbation becomes

$$\dot{x} = f(t,x) + G(t,x)\psi(t,x) + G(t,x)[v + \delta(t,x,\psi(t,x)+v)] \tag{4.58}$$

Calculating time derivative of Lyapunov function along the trajectories of (4.58)

$$\dot{V} = \frac{\partial V}{\partial t} + \frac{\partial V}{\partial x}(f + G\psi) + \frac{\partial V}{\partial x}G(v+\delta) \le -\alpha_3(\|x\|) + \frac{\partial V}{\partial x}G(v+\delta) \tag{4.59}$$

Setting $w^T = \frac{\partial V}{\partial x}(G)$ eq. (4.59) becomes

$$\dot{V} \le -\alpha_3(\|x\|) + w^T v + w^T \delta \tag{4.60}$$

The first term of (4.60) represents nominal system in closed loop configuration. Second term represents effect of control 'v' on $\dot{V}$ and the third term is the effect of the uncertainty on $\dot{V}$.

Since the matching condition for the uncertainty is considered therefore uncertainty term appears at identical positions where control 'v' presents. Now the uncertainty effect that destabilizes $\dot{V}$ can easily be cancelled.

Supposing control 'v' such that $w^T v + w^T \delta \leq 0$ and suppose the inequality (4.57) is satisfied with $\|\cdot\|_2$

$$\left\|\delta(t, x, \psi(t, x) + v\right\|_2 \leq \rho(t, x) + \kappa_0 \left\|v\right\|_2, \ 0 \leq \kappa_0 \leq 1 \tag{4.61}$$

Since,

$$w^T v + w^T \delta \leq \left\|w\right\|_2 \left\|\delta\right\|_2 \leq w^T v + \left\|w\right\|_2 \left[p(t, x) + \kappa_0 \left\|v\right\|_2 \right] \tag{4.62}$$

Now taking,

$$v = -\eta(t, x). \frac{w}{\left\|w\right\|_2} \tag{4.63}$$

Considering a nonnegative function η , we obtain

$$w^T v + w^T \delta \leq -\eta \left\|w\right\|_2 + \rho \left\|w\right\|_2 + \kappa_0 \eta \left\|w\right\|_2 = -\eta (1 - \kappa_0) \left\|w\right\|_2 + \rho \left\|w\right\|_2 \tag{4.64}$$

Now selecting $\eta(t, x) \geq \rho(t, x) / (1 - \kappa_0) \ for \ all (t, x) \in [0, \infty) \times D$ results

$$w^T v + w^T \delta \leq -\rho \left\|w\right\|_2 + \rho \left\|w\right\|_2 = 0 \tag{4.67}$$

Hence using the control input of (4.63), $\dot{V} \leq 0$ for system with perturbation described in (4.58).

The control law of (4.63) is discontinuous function of states of the system. The easy and practical continuous control law is proposed below,

$$v = \begin{cases} -\eta(t,x).\dfrac{w}{\|w\|_2}, & if \ -\eta(t,x)\|w\|_2 \geq \varepsilon \\ -\eta^2(t,x)(w/\varepsilon), & if \ -\eta(t,x)\|w\|_2 < \varepsilon \end{cases} \tag{4.68}$$

It is proposed in the light of the theorem 14.3 and corollary 14.1 [57]

When η satisfies (4.71), the feedback control law of (4.68) will work in the region $\eta\|w\|_2 < \varepsilon$.

$$v = -kw \tag{4.69}$$

having $k = \dfrac{\eta_0^2}{\varepsilon}$. Here $\varepsilon < \min\left\{\dfrac{2(1-\kappa_0)}{\rho_1^2}, \dfrac{2\alpha_3(r).\alpha_1(r)}{(1-\kappa_0).\alpha_2(r)}\right\}$

This high gain feedback control will stabilize the origin of the system with uncertainty when (4.70)-(4.72) are satisfied.

$$\alpha_3\left(\|x\|_2\right) \geq \phi^2(x) \tag{4.70}$$

$$\eta(t,x) \geq \eta_0 > 0 \tag{4.71}$$

$$\rho(t,x) \leq \rho_1\phi(x) \tag{4.72}$$

Now to satisfy the equations (4.70)-(4.72),

$$\eta = 1 + \frac{\rho_1 \|x\|_2}{(1-\kappa_0)} \tag{4.73}$$

$$w^T = 2x^T PB \tag{4.74}$$

$$\varepsilon < \min\left\{ \frac{2(1-\kappa_0)}{\rho_1^2}, \frac{2r^2.\lambda_{\min}(P)}{(1-\kappa_0).\lambda_{\max}(P)} \right\} \tag{4.75}$$

Assumptions of Corollary 14.1 and Theorem 14.3 can be fulfilled by choosing $\alpha_1(r) = \lambda_{\min}(P)r^2, \alpha_2(r) = \lambda_{\max}(P)r^2, \alpha_3(r) = r^2, \phi(x) = \|x\|_2 \; and \; a = r.$

For the control of external part of the normal form of the AUV system described in (4.38),

$$\lambda_{\min}(P) = 0.73$$

$$\lambda_{\max}(P) = 2.73$$

$$w^T = 2\xi_1 + 3.46\xi_2$$

Let $r = 1$, $\kappa_0 = 0.5 \; and \; \rho_1 = 2$

Solving for ε

$$\varepsilon < \min\{0.25, 1.07\}$$

From (4.73), $\eta_0 = 1$

Considering $\varepsilon = 0.5 < 1.07$ for k. Then K=2

Now the control input of (4.69) becomes,

$$v = -4\xi_1 - 6.92\xi_2 \tag{4.76}$$

The control input of (4.76) will exponentially stabilize the system with uncertainty of (4.58).

4.5.1 Simulations

Depth Response:

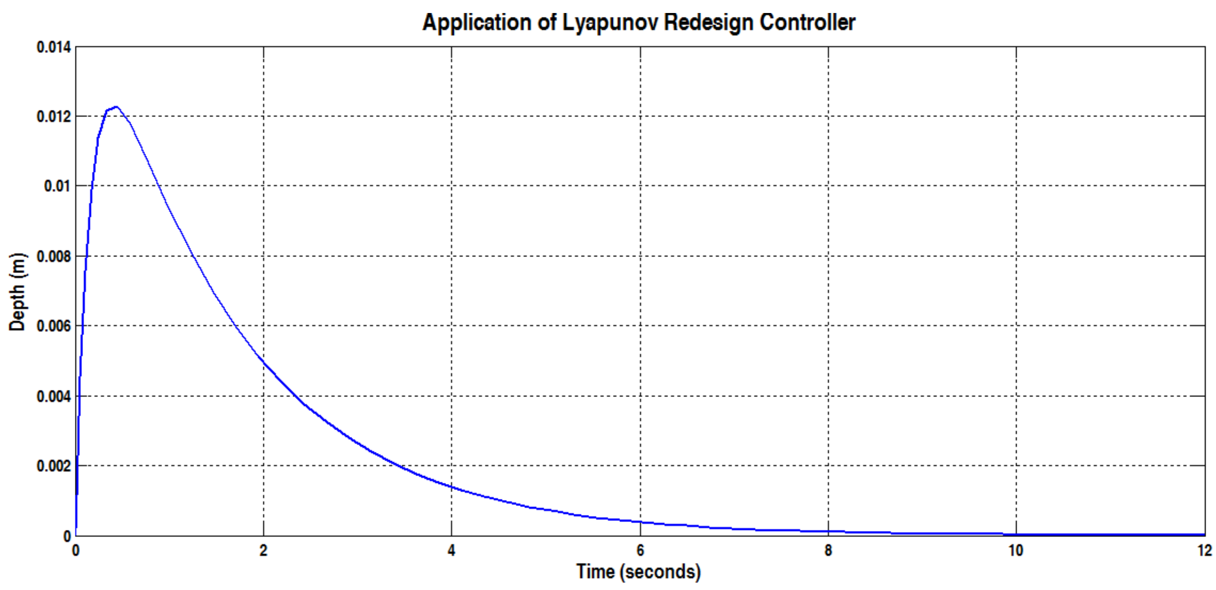

Figure 4.5 Depth response on application of Lyapunov Redesign Controller

It can be seen in fig. (4.5) that the feedback controller designed with the Lyapunov Redesign technique stabilizes the system without uncertainty in almost 9 seconds with an overshoot of 1.2% in depth.

Controller Response:

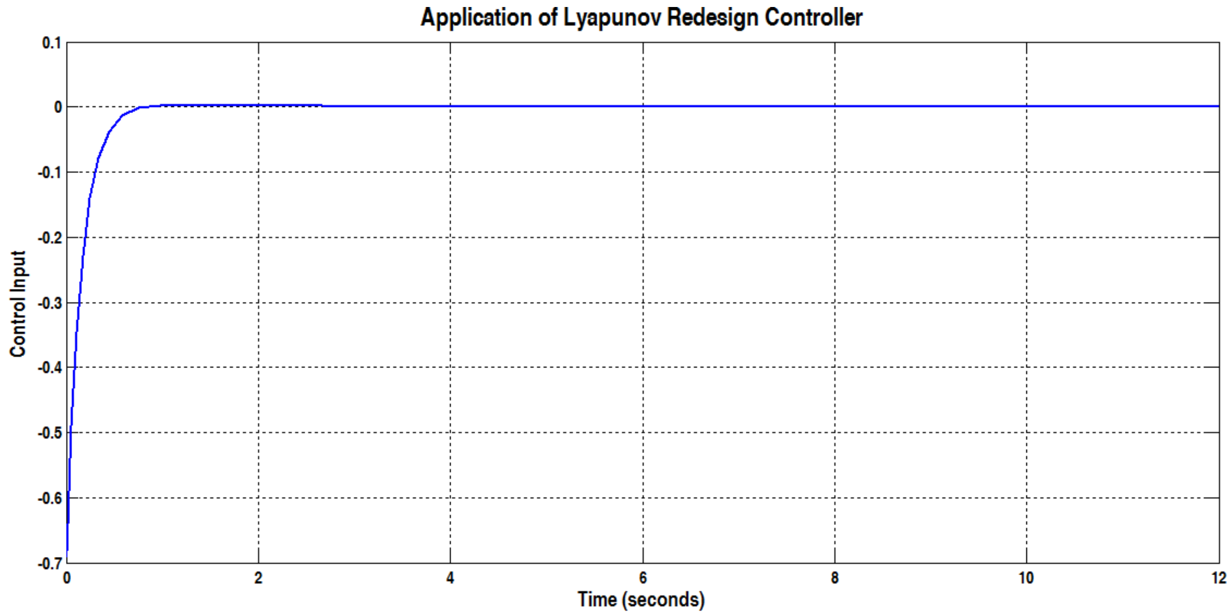

0

Figure 4.6 Lyapunov Redesign Controller Response

The controller input takes an effort of 0.7 to stabilize the system and then keeps the system stable in steady state.

4.5.2 Uncertainty Rejection in Input by the controller:

To check the uncertainty rejection quality of controllers, a random uncertain signal of varying magnitude within 0.1 magnitudes is added in the controller input.

Depth Response against uncertainty in input:

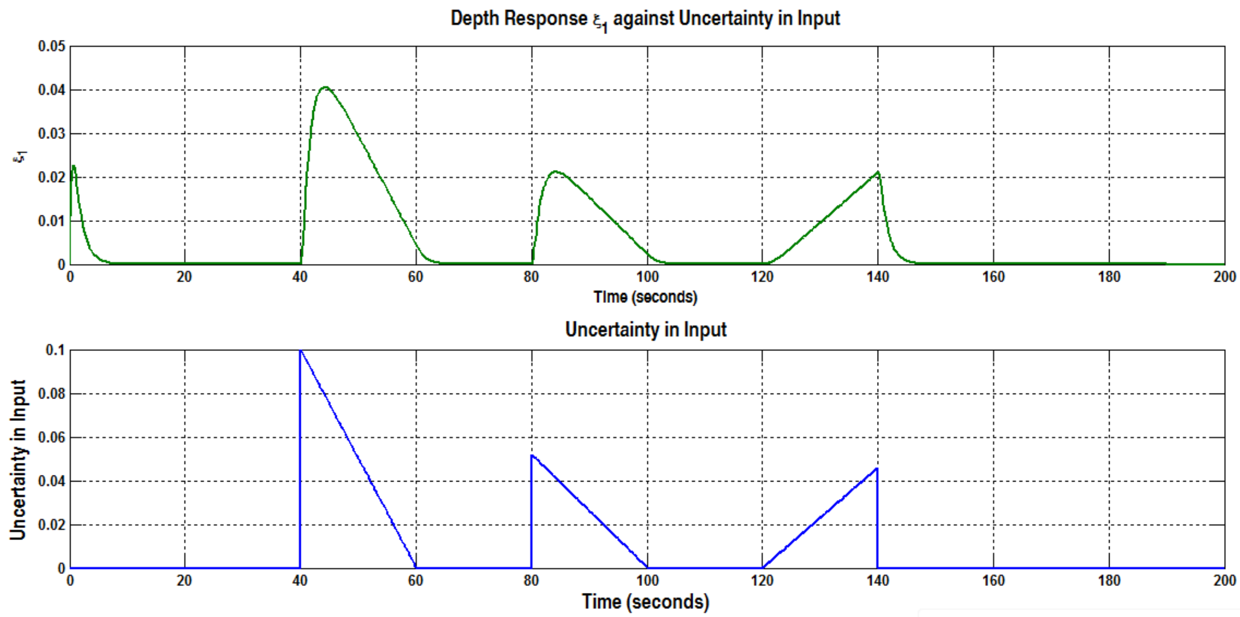

Figure 4.7 Uncertainty rejections in Depth response

It is observed that the effect of uncertainty in input effects the depth response of AUV but the lyapunov redesign based controller is suppressing its effect. It can be seen in the above simulation that for 10% uncertainty in input, the depth response suppress its effect efficiently within 4% and removes them after some time.

4.6 Inverse Optimal Control

Inverse Optimal Control is an indirect approach in solving optimal control problems. In this technique, a nonlinear dynamical model of a system under consideration is used to establish control law that ensures stabilization to the system. Due to the complex and lengthy calculations of the HJB equations to get an optimal solution, this Inverse optimal control is suitable for the dynamical systems of higher order. The Inverse optimal control strategy used in this chapter is based on existence of a CLF. The CLF is used for testing the capability of the system to be feedback stabilizable. It means that on the application of any control input v(x,t) the X states of the systems can be brought to the zero state. E.D Sontag and Z. Artstein developed the theory and application of CLF in 1980's and 1990's [58].

An ordinary Lyapunov function V(x) is used to test the stability (more specifically the asymptotic stability) of a dynamical system without applying any inputs. This test checks the dynamical system starting from a state other than origin in a domain D remains in that domain. In case of asymptotic stability, the dynamical system will return to origin.

On the other hand CLF is a Lyapunov function for a dynamical system with control inputs. The CLF tests the feedback stabilizability of a system considering existence of a control input $v(x,t)$ such that the system states can be brought to the origin on application of that control input.

Consider a dynamical system of the form

$$\dot{x} = f(x, v) \tag{4.77}$$

Where state vector $x \in \mathbb{R}^n$ and control input vector $v \in \mathbb{R}^m$. It is desired to feedback stabilize the system at origin (x=0).

Definition 4.1 *A CLF is a function V(x) that in domain D, where* $D \to \mathbb{R}$ *is positive definite and continuously differentiable such that we can find a control input 'v' for each state 'x' that will reduce the energy of the system. Mathematically,*

$$\dot{V}(x,u) = \frac{\partial V}{\partial x} f(x,v) < 0 \qquad \forall x \neq 0, \exists v \tag{4.78}$$

If there is a stabilizing feedback control input that stabilizes the states of the dynamical system, then that dynamical system has a differentiable CLF satisfying (4.77)[59].

For the designing and application of an Inverse optimal control, a CLF for the system under consideration must be known. For this reason, the following conditions for the existence of a CLF must be fulfilled by any positive definite lyapunov function V(x),

Theorem 4.2 *A continuously differentiable positive definite function V(x) is a CLF for a system if*

$$\left\{ \frac{\partial V}{\partial x} g(x) = 0 \ \ for \ x \in D, x \neq 0 \Rightarrow \dot{V}(x) < 0 \right\} \tag{4.79}$$

where $D \subset R^n$ [53].

- **Condition for CLF existence**

This condition needs derivative of any positive definite function considered as lyapunov function should must be less than zero. So we have to prove $\dot{V}(x) < 0$ that is $\inf_v \left[\frac{\partial V(x)}{\partial x} f(x, v) \right] < 0 \quad \forall x \neq 0$. For this purpose, the Artstein's theorem is used, that states

Theorem 4.3 *A dynamical system has a differentiable CLF if and only if there exists a regular stabilizing feedback controller v(x)*

According to theorem 4.3, if there is a stabilizing feedback controller for a dynamical system then that system has a differentiable CLF. Moreover V(x) indicates existence of CLF for given system is equal to existence of a control v=k(x) that is asymptotically feedback stabilizing control.

To make a stabilizing controller, the following need to be solved,

$$k(x) = \arg\min_v \left\{ |v| : \frac{\partial V}{\partial x}\left(f(x) + g(x)v \right) \leq -\sigma(x) \right\} \tag{4.80}$$

where $\sigma(x)$ is positive definite.

k(x) is to be constructed such that v=k(x) corresponds to an optimal control problem.

$$J = \int_0^\infty \left(q(x) + v^2 \right) dt \tag{4.81}$$

Choosing

$$\sigma(x) = \sqrt{\left(\frac{\partial V}{\partial x}.f(x)\right)^2 + q\left(\frac{\partial V}{\partial x}.g\right)^2} \tag{4.82}$$

Solving for 'v' from $\frac{\partial V}{\partial x}(f(x)+g(x)v) = -\sigma(x)$

$$k(x) = \begin{cases} -\dfrac{\frac{\partial V}{\partial x}.f(x)+\sigma(x)}{\frac{\partial V}{\partial x}.g} & for\ \frac{\partial V}{\partial x}.g \neq 0 \\ 0 & for\ \frac{\partial V}{\partial x}.g = 0 \end{cases} \tag{4.83}$$

The above described control law is continuous everywhere except x=0.

Using lie-derivatives notations,

$$L_f V \triangleq \frac{\partial V}{\partial x}.f(x)$$

$$L_g V \triangleq \frac{\partial V}{\partial x}.g(x)$$

The HJB equation for the optimal control is described as,

$$\min_v \left\{ \frac{1}{2}\left(q(x)+v^2\right) + \frac{\partial V^*}{\partial x}\left(f(x)+g(x)v\right) \right\} = 0 \tag{4.84}$$

where $V^*(x)$ represents value function. $V^*(0) = 0$

$$v + \frac{\partial V^*}{\partial x} g(x) = 0$$

$$v = -L_g V^* \tag{4.85}$$

Solving HJB equation of (4.84) by using ‘v’ of (4.85)

$$\Rightarrow \frac{1}{2} q(x) - \frac{1}{2}\left(L_g V^*\right)^2 + \left(L_f V^*\right)\left(L_g V^*\right) + \left(L_g V^*\right)^2 = 0$$

Solving the above quadratic equation in terms of $L_g V^*$

$$L_g V^* = -\frac{L_f V^* + \sqrt{\left(L_f V^*\right)^2 - q\left(L_g V^*\right)^2}}{L_g V^*} \tag{4.86}$$

Considering the selected lyapunov function $V(x) = V^*(x)$ that minimizes the cost function, then

$$k(x) = -L_g V^*(x) \tag{4.87}$$

is the optimal controller.

Considering a positive definite quadratic Lyapunov function $V(\xi) = \frac{1}{2}\xi_1^2 + \frac{1}{2}\xi_2^2$

$$\frac{\partial V}{\partial \xi} = [\xi_1 \quad \xi_2] \tag{4.88}$$

We have from the external part of the normal form of the diving model of AUV system of (4.26)

$$f(x) = \begin{bmatrix} \xi_2 \\ 0 \end{bmatrix} \text{ and } g = \begin{bmatrix} 0 \\ 1 \end{bmatrix}$$

Calculating the lie derivatives of f(x) and g

$$L_f V = \xi_1 \xi_2$$

$$L_g V = \xi_2$$

Now considering the selected Lyapunov function as a CLF and $q(\xi) = \xi_1^2 - \xi_2^2$, (4.87) becomes,

$$v = k(\xi) = -\xi_1 - \xi_2 \tag{4.89}$$

4.6.1 Stability Analysis

To prove the stability of the inverse optimal control, the definition 4.1 and theorem 4.2 are used that the time derivative of selected quadratic lyapunov function is negative definite.

$$\dot{V}(\xi) = \xi_1 . \dot{\xi}_1 + \xi_2 . \dot{\xi}_2$$

$$\Rightarrow \dot{V}(\xi) = \xi_1 \xi_2 + \xi_2 v$$
$$\Rightarrow \dot{V}(\xi) = \xi_1 \xi_2 + \xi_2 (-\xi_1 - \xi_2)$$
$$\Rightarrow \dot{V}(\xi) = \xi_1 \xi_2 - \xi_1 \xi_2 - \xi_2^2$$

$$\dot{V}(\xi) = -\xi_2^2 \quad , \quad \dot{V}(\xi) < 0 \tag{4.90}$$

So it is proved that GAS with the use of selected lyapunov function.

4.6.2 Simulations

Depth response Comparison of Lyapunov Redesign and Inverse Optimal Controllers

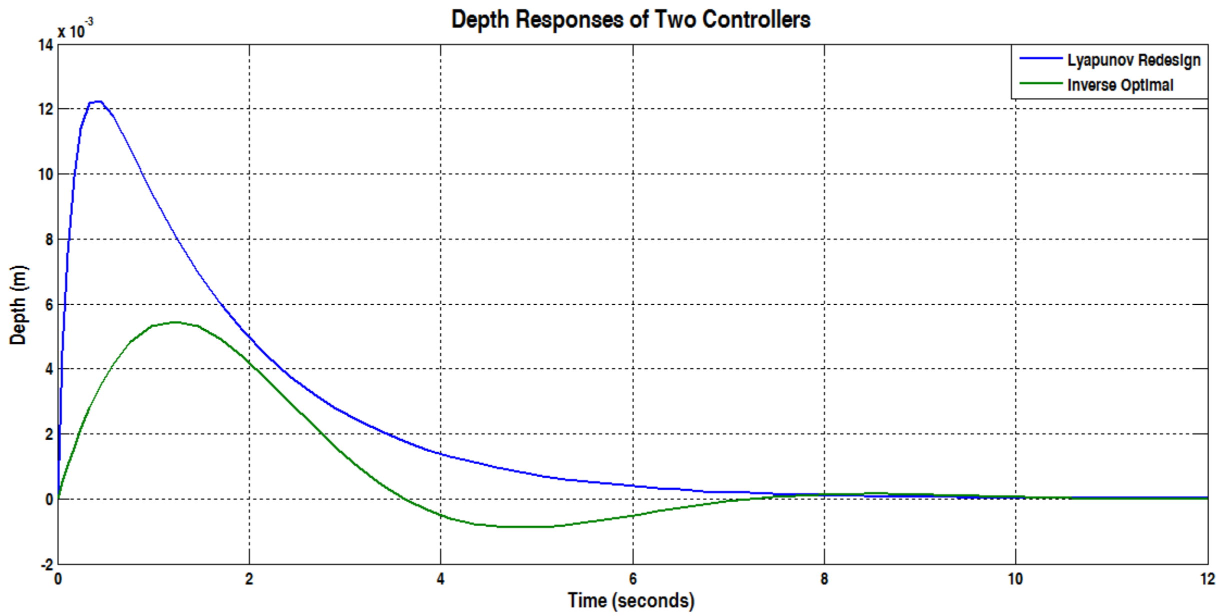

Figure 4.8 Depth responses of Inverse Optimal and Lyapunov Redesign Controllers

It is observed from fig.(4.8) that both of the controllers stabilizing the depth of AUV in 8 seconds. Since the overshoot in transient response of the Lyapunov Redesign controller is 1.2%, the Inverse Optimal Controller is better with less than 0.6% overshoot.

Control Input responses of two controllers:

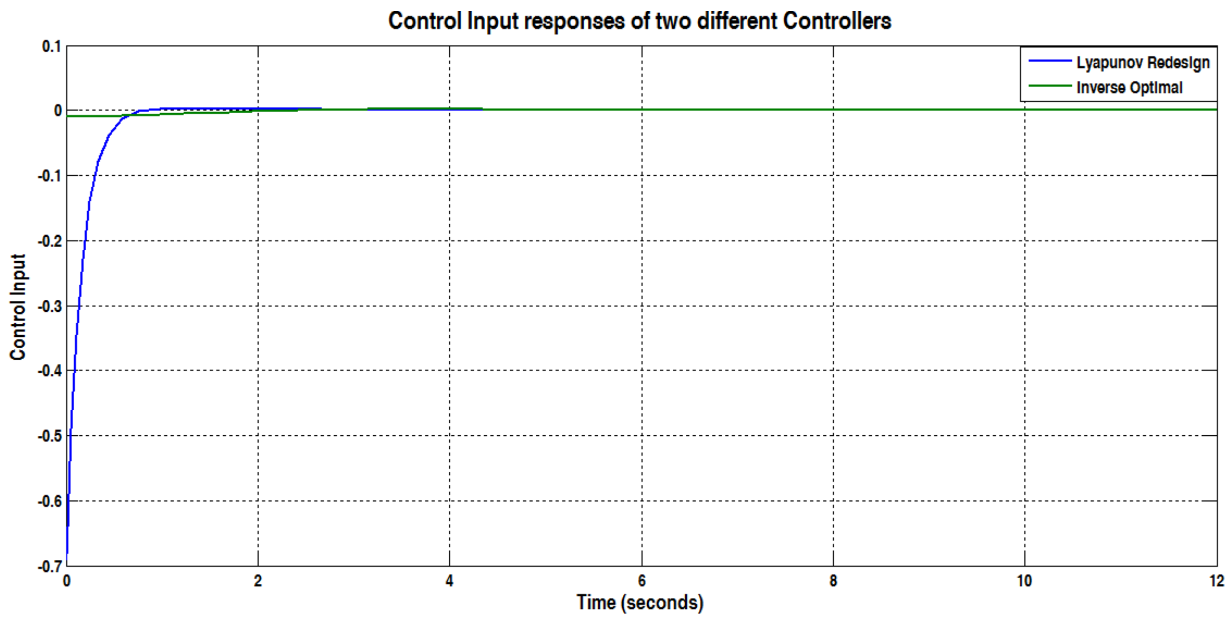

Figure 4.9 Control Input response of the controllers

It can be seen clearly in fig.(4.9) that the Inverse Optimal Controller has used very low amount of controller input to stabilize the depth of AUV as compared to Lyapunov Redesign Controller.

4.7 Trajectory tracking using Robust Optimal Control

A time varying reference is selected as AUV depth tracking signal. The controller used for tracking is the combination of SMC and Inverse optimal control to achieve optimal robustness. The structure of the proposed controller is as follows,

$$v = -(\xi_1 - \xi_d) - \xi_2 - sat\left(\frac{0.5(\xi_1 - \xi_d) + 1.5\xi_2}{\varepsilon}\right) \tag{4.91}$$

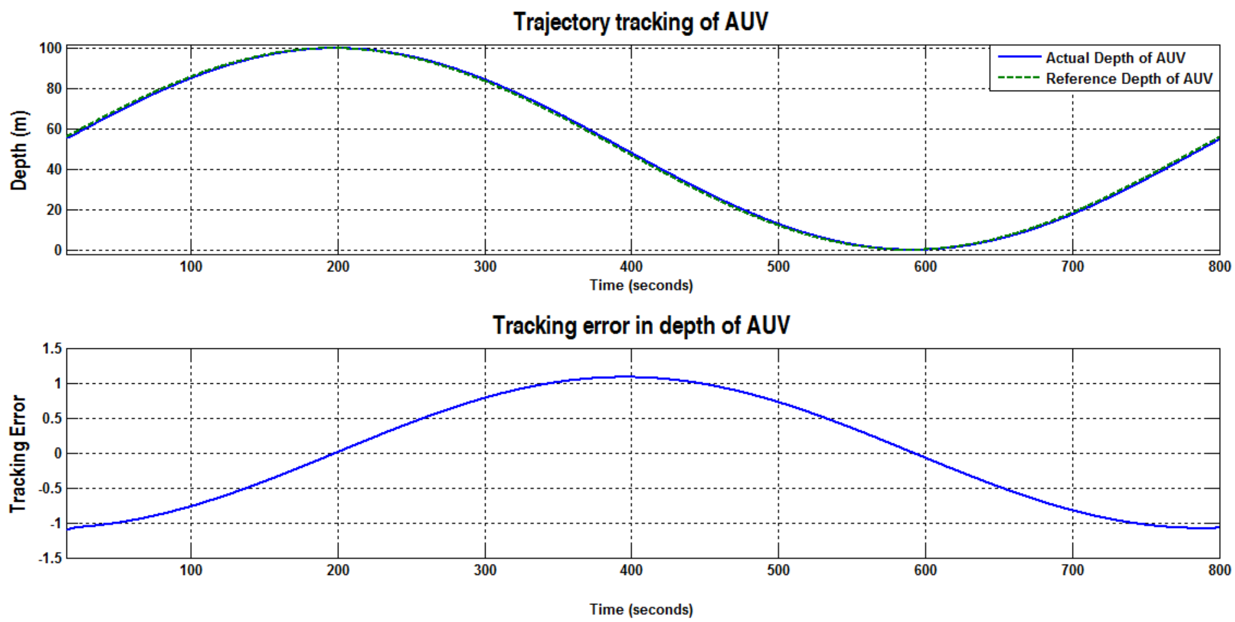

Figure 4.10 Trajectory tracking of AUV with tracking error under robust optimal controller

It is concluded from the simulations shown in fig. (4.10) that the proposed optimal controller is tracking the varying reference trajectory efficiently. The maximum error limit in tracking a trajectory is within the bound of ± 1%.

4.8 Output Feedback Controller

In this section, we design controller using Output Feedback technique and incorporating an HGO which is considered an important milestone in the design of nonlinear observers for unmeasured system states while designing Output Feedback controllers because of its performance recovery feature like state feedback controller and system convergence to that of the actual nonlinear system. To design the output feedback controller, the first step is to design a robust observer for the states estimation. The uniqueness in this section is the application of the Inverse Optimal Controller based Output Regulation control using HGO to emulate system behavior.

To investigate the order of the observer to be designed for the system, systems relative degree ρ needs to be calculated. For this purpose, output of the system is differentiated for a number of times unless an equation is produced showing input.

Since output of the system is $y = x_1$, differentiating it,

$$\dot{y} = \dot{x}_1 = x_3 \cos(x_2) \tag{4.92}$$

No input comes up. So again differentiating (4.92),

$$\ddot{y} = \ddot{x}_1 = \frac{d}{dx}(x_3 \cos(x_2)) = -x_3 \sin(x_2).\dot{x}_2 + \cos(x_2) \tag{4.93}$$

Where $\dot{x}_2$ contains the control input. Since the differentiating of the output is carried two times, so the relative degree $\rho = 2$. Therefore an observer/estimator is required to implement a real time controller.

In view of the High Gain Observer design method, the Observer for system becomes:

$$\begin{Bmatrix} \dot{\hat{\xi}}_1 = \hat{\xi}_2 + h_1(y - \hat{\xi}_1) \\ \dot{\hat{\xi}}_2 = h_2(y - \hat{\xi}_1) + v \end{Bmatrix} \tag{4.94}$$

Where the gains are chosen such that,

$$\begin{bmatrix} h_1 \\ h_2 \end{bmatrix} = \begin{bmatrix} 2/\varepsilon \\ 1/\varepsilon^2 \end{bmatrix} \tag{4.95}$$

where‘ε’ is the design parameter. Implementing HGO as output feedback controller is proven to recover the controller performance designed on state feedback technique by choosing appropriate gains of HGO. This can be accomplished by selecting the value of design parameter $'\varepsilon'$ small enough that reduces the error of state estimation down to zero as $'\varepsilon'$ reaches zero. The selection of small value of design parameter $'\varepsilon'$ leads to limited time large overshoot in the transient response of the observer. This is referred as ‘peaking phenomenon’ and can be eliminated by saturating the response of the observer during the short transient period that contains peaking.

Therefore, using HGO for output feedback controller and the estimated states from the observer forms the overall feedback inverse optimal controller from (4.24) and (4.89) results in (4.96):

$$\delta_s = \overset{\frown}{\delta}_s + v = \overset{\frown}{\delta}_s - \hat{\xi}_1 - \hat{\xi}_2 \tag{4.96}$$

4.9 Theorem 3

Closed loop system of diving model of AUV (4.22) is considered for stabilization and designing the controller for output feedback case (4.96). Suppose the state feedback control design in (4.96) for the closed loop system has an asymptotically stable origin. The region of attraction of origin is R. Let W as any compact subset inside the boundary of R and X as any compact subset inside the boundary of R_0 . Then,

- $\varepsilon_1^* > 0$ exists s.t for each and every $\varepsilon_1^* \geq \varepsilon \geq 0$ the diving model of AUV's closed loop system has solutions starting in W x X and bounded for all $t > 0$ on application of state feedback $'\xi(t)'$ with and without observer $'\hat{\xi}(t)'$.

- For some $w > 0$, $\varepsilon_2^* > 0$ & $T_2 > 0$ exists having dependency upon $'w'$ s.t for each and every $\varepsilon_2^* \geq \varepsilon \geq 0$,the diving model of AUV's closed loop system has solutions starting in W x X and bounded for all $t > T_2$ on application of state feedback controller with and without observer satisfying

$$\|\xi(t)\| \leq w \qquad \& \qquad \|\hat{\xi}(t)\| \leq w \qquad \forall\ t \geq T_2$$

- For some $w > 0$, $\varepsilon_3^* > 0$ exists having dependency upon $'w'$ s.t for each and every

  $\varepsilon_3^* \geq \varepsilon \geq 0$, the closed loop solutions of the diving model AUV system, starting in W x X

  satisfies

$$\|\xi(t) - \xi_r(t)\| \leq w \qquad for\ all\ \ t \geq 0$$

  here X_r is solution of (4.89) starting from the initial conditions X(0).

- Now considering $f(\xi)$ as continuously differentiable in the vicinity of origin of (4.89)

  that is exponential stable, $\varepsilon_4^* > 0$ exists s.t for each and every $\varepsilon_4^* \geq \varepsilon \geq 0$, the diving

  model of AUV's closed loop system has exponentially stable origin having W x X as a

  subset of its R (the region of attraction).

4.10 Proof

Considering the objectives of this work and with suitable modifications, this proof tracks general outline explained in [60]. It explains that the state feedback controller performance can be recovered by an output feedback controller for small values of $'\varepsilon'$. The performance recovery is divided into three steps. The first step is the exponential stability performance recovery. The second step includes the recovery of a compact set in the interior of the region of attraction.

Third step is, with the passage of time as the time tends to ‘0’, the output feedback performance approaches the state feedback performance.

4.11 Remarks

It is well known that with local exponential stability if a controller based on state feedback approach attains semi global or global stabilization then for suitable minor value of 'ε', the controller designed on output feedback technique attains semi global stabilization.

4.12 Simulations of Inverse Optimal Controller with Reduced Order High Gain Observer

The simulation with and without HGO using different parametric values of 'ε' under Inverse Optimal Control are shown in figure below:

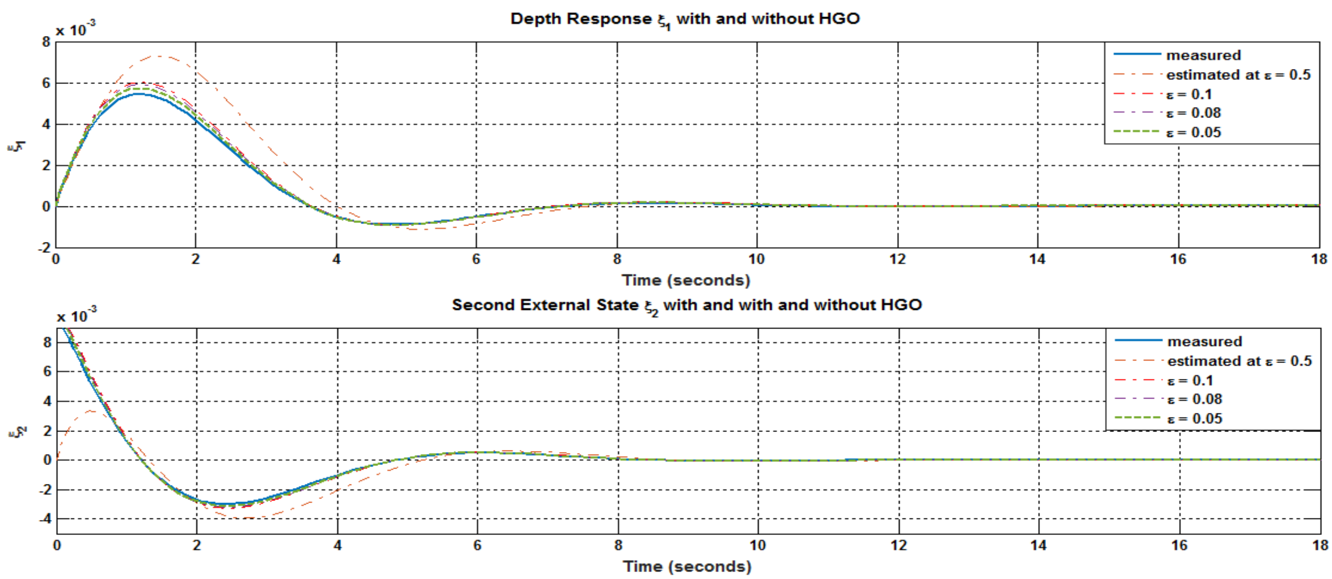

Figure 4.11 System states responses with and without HGO using different design parameter values

It is concluded from the simulations that the states of the systems are estimated more accurately with the HGO having design parameter '$\varepsilon = 0.005$'.

4.13 Simulations of SMC with Reduced Order High Gain Observer

Using the HGO dynamics presented in (4.94)

$$\begin{cases} \dot{\hat{\xi}}_1 = \hat{\xi}_2 + h_1(y - \hat{\xi}_1) \\ \dot{\hat{\xi}}_2 = h_2(y - \hat{\xi}_1) + v \end{cases}$$

And the SMC proposed as in (4.48)

$$v = -sat\left(\frac{0.5\hat{\xi}_1 + 1.5\hat{\xi}_2}{\varepsilon}\right)$$

Simulations with and without HGO using different values of 'ε' are shown in Fig 4.12:

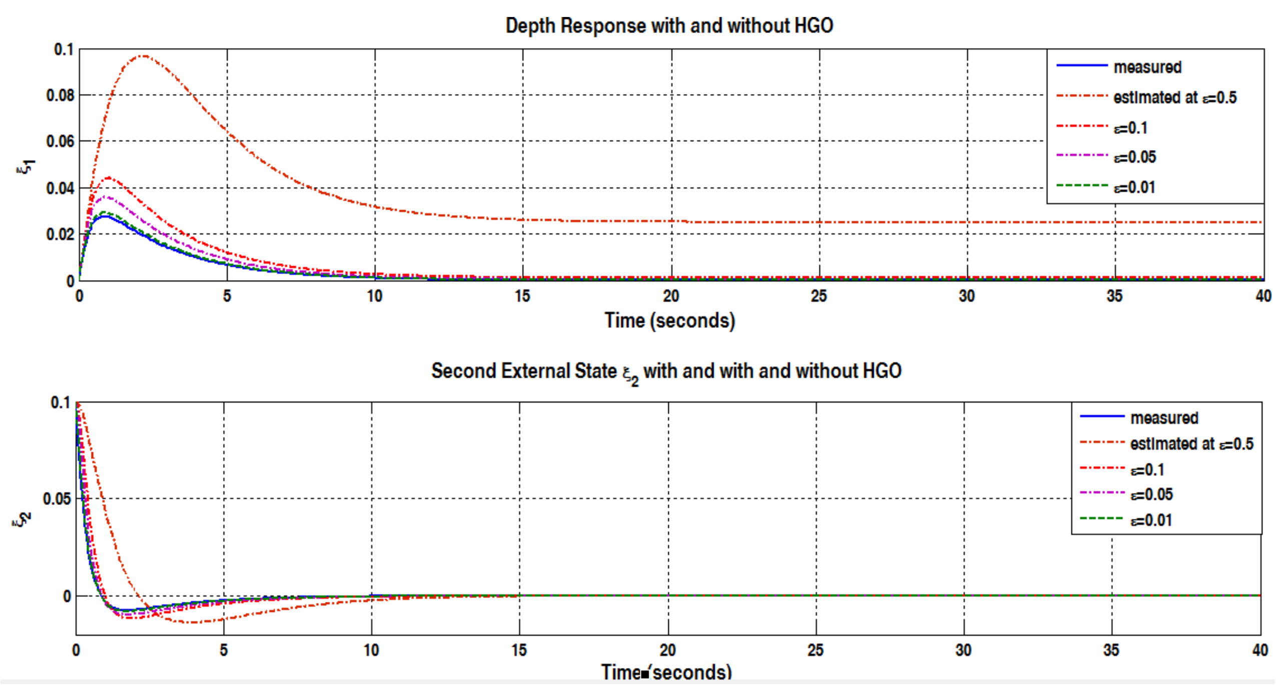

Figure 4.12 System states responses with and without HGO using different design parameter values

It is concluded from the simulations that the states of the systems are estimated more accurately with HGO having the design parameter '$\varepsilon = 0.001$'.

4.14 Simulations of SMC with Inverse Optimal Control using Reduced Order High Gain Observer

The simulation with and without HGO using different parametric values of 'ε' under robust optimal control are shown in figure below:

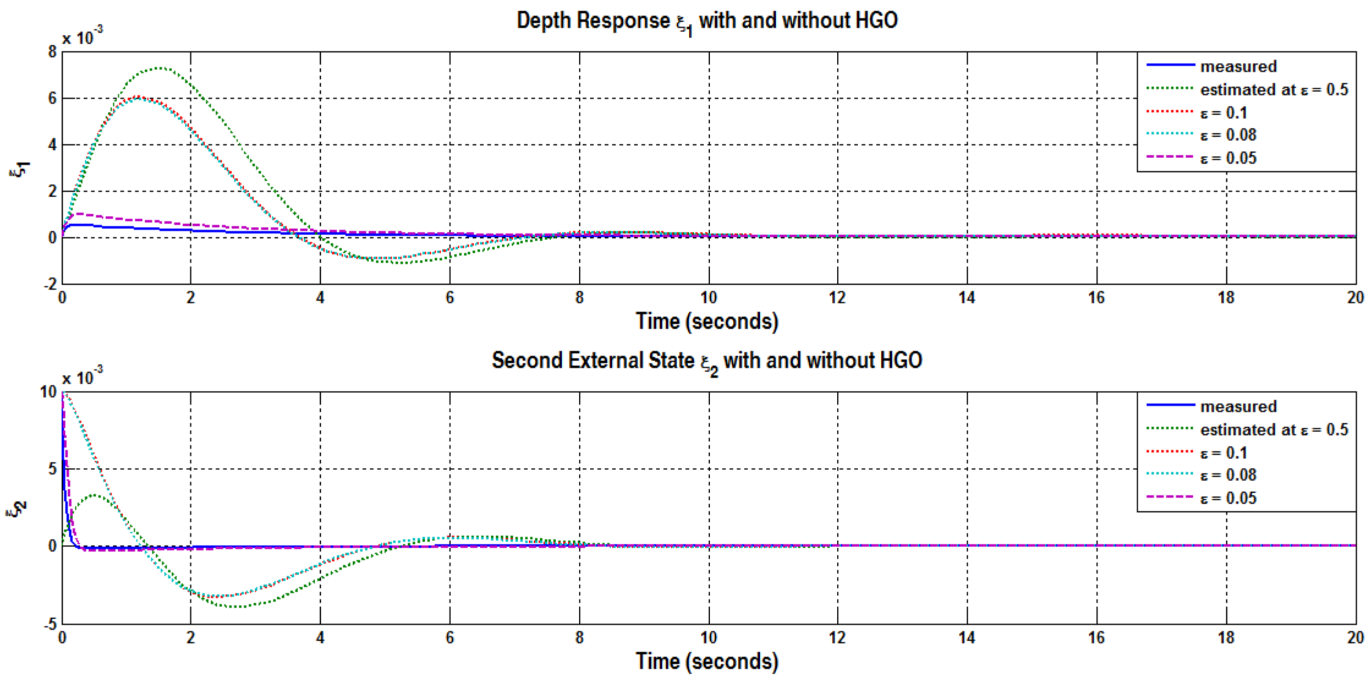

Figure 4.13 System states responses with and without HGO using different design parameter values

It is observed from the simulations that the states of the systems are estimated more accurately with HGO having the design parameter '$\varepsilon = 0.05$'.

4.15 State Feedback Controller with Full Order High Gain Observer

In order to estimate all of the states of the system in normal form, a full order HGO is technique is taken into account instead of reduced order HGO presented in above sections.

The structure of the full order HGO for the normal form of the AUV system as presented in (4.22) is

$$\begin{aligned}
\dot{\hat{\eta}}_1 &= C_1\hat{\xi}_2 \sec\hat{\eta}_1 + C_2 \tan\hat{\eta}_1 - C_3\hat{\eta}_2 + \alpha_1(\xi_1 - \hat{\xi}_1) \\
\dot{\hat{\eta}}_2 &= C_4\hat{\xi}_2 \sec\hat{\eta}_1 + C_5 u \tan\hat{\eta}_1 - C_6\hat{\eta}_2 + \alpha_2(\xi_1 - \hat{\xi}_1) \\
\dot{\hat{\xi}}_1 &= \hat{\xi}_2 + \alpha_3(\xi_1 - \hat{\xi}_1) \\
\dot{\hat{\xi}}_2 &= v + \alpha_4(\xi_1 - \hat{\xi}_1)
\end{aligned} \tag{4.97}$$

Where

$$\begin{aligned}
\alpha_1 &= a_1/\varepsilon \\
\alpha_2 &= a_2/\varepsilon^2 \\
\alpha_3 &= a_3/\varepsilon^3 \\
\alpha_4 &= a_4/\varepsilon^4 \\
y &= \xi_1
\end{aligned}$$

Here the coefficients are selected such that the polynomial $s^4 + \alpha_1 s^3 + \alpha_2 s^2 + \alpha_3 s + \alpha_4 = 0$ has all its roots in the complex left half plane. So coefficients are selected such that, $a_1 = 1, a_2 = 2, a_3 = 3, a_4 = 4$.

The controller used in this part is the nominal state feedback controller, $v = -0.3\hat{\xi}_1 - 0.8\hat{\xi}_2$

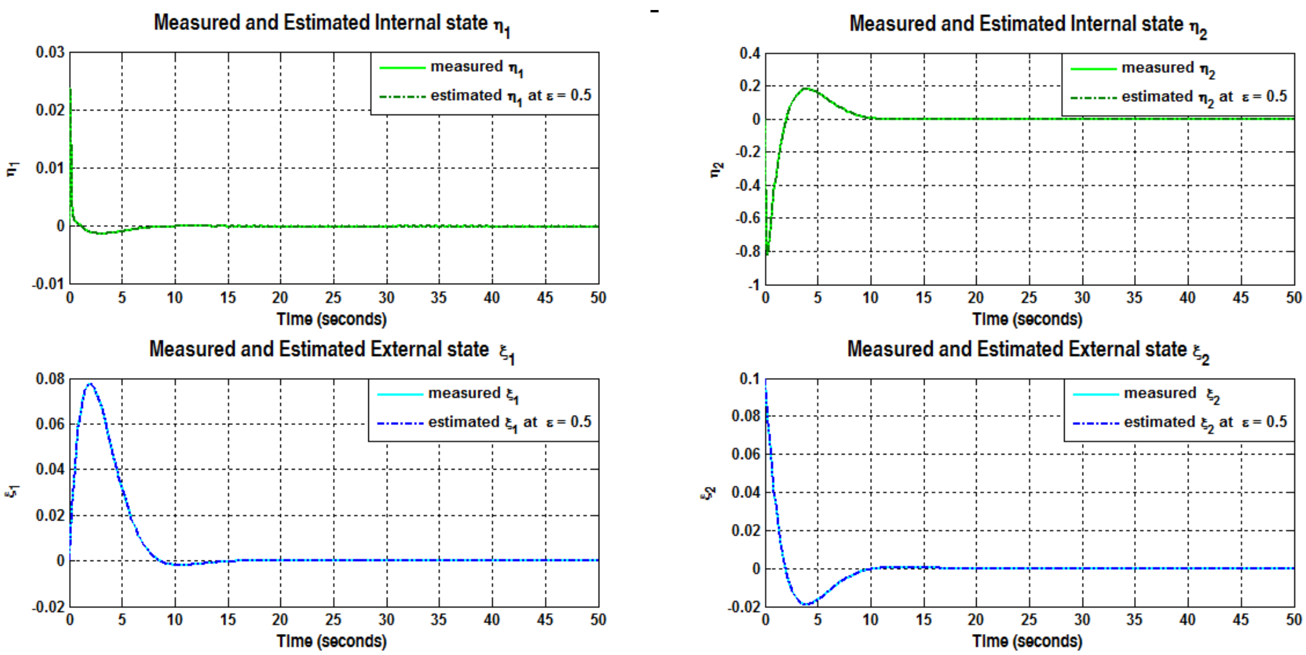

Figure 4.14 System states measured responses versus estimated ones using state feedback controller

The full order HGO designed for the nonlinear system is efficiently estimating the system states as shown in figure (4.14). The whole system on application of state feedback control is stabilizing in 15 seconds.

4.16 SMC+Inverse Optimal Controller with Full Order HGO

The controller used in this part is SMC with Inverse Optimal Controller

$$v = -\hat{\xi}_1 - \hat{\xi}_2 - sat\left(\frac{-0.5\hat{\xi}_1 - 1.5\hat{\xi}_2}{0.5}\right)$$

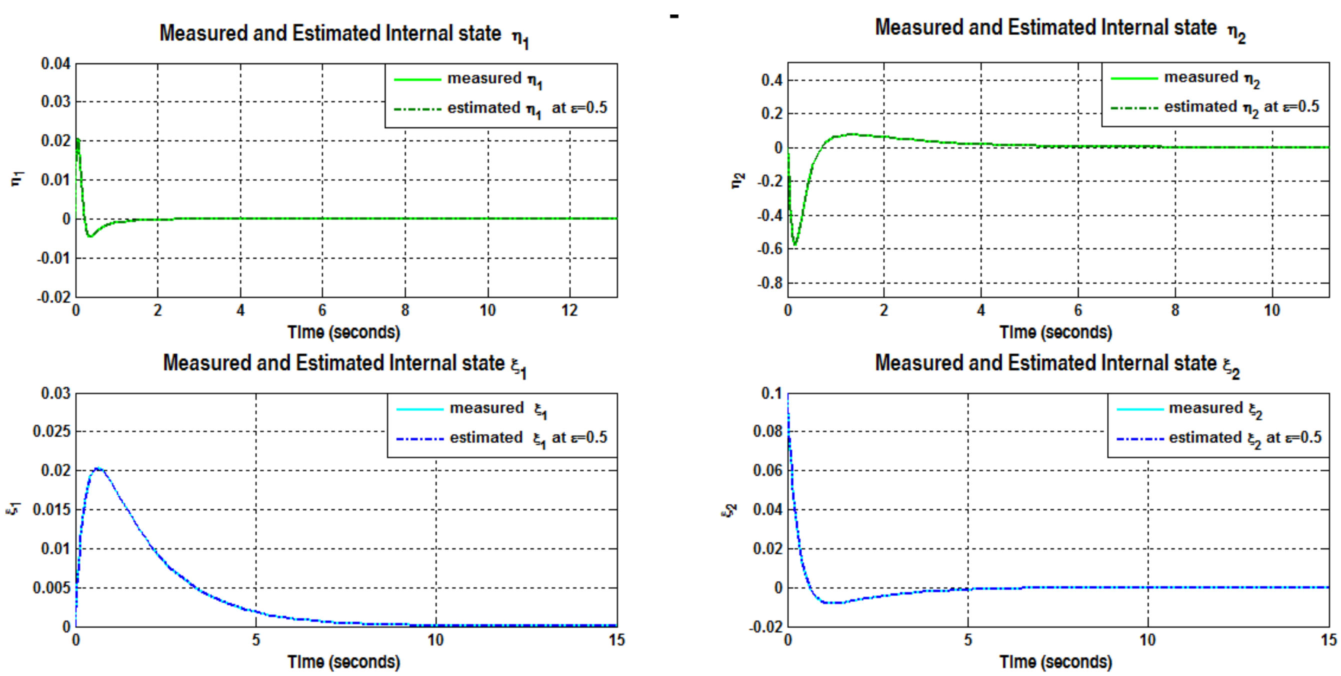

Figure 4.15 System states measured responses versus estimated ones using SMC with Inverse Optimal controller

The full order HGO designed for the nonlinear system is efficiently estimating the system states as shown in figure (4.15). The whole system on application of SMC with Inverse Optimal control is stabilizing in 10 seconds.

Chapter

5

CONCLUSION AND FUTURE RECOMMENDATIONS

5.1 Conclusion

This thesis addresses optimal and stabilization problem of a nonlinear dynamical model of AUV and its solution. Linear control techniques, linear state-feedback and optimal controllers are designed and implemented on nonlinear model of AUV. Full state linear observers for both of the controllers are designed and implemented.

Then a nonlinear state feedback stabilizing control law is designed to stabilize nonlinear model of AUV. SMC is then designed for robust control. The nonlinear optimal control law is then designed using the Inverse Optimal Control design approach based on the existence of a Control Lyapunov Function and use of slight variation of Sontag's Formula. A quadratic energy function is chosen as lyapunov function in order to inspect the asymptotic stability of the system under consideration. These nonlinear controllers are then compared with respect to their performances and costs in simulations. A varying reference depth tracking is also achieved meeting desired performance requirements. A controller based on output feedback is then calculated so as to achieve stability of optimal and robust feedback controller under variations of states signals from sensors. Reduced and full order HGO's are designed to meet the requirements. Analytical proofs, lyapunov stability analysis with extensive graphical results have been incorporated to validate the proposed controller's performances.

5.2 Future Recommendations

Future recommendations include optimal and robust control of steering and diving plane, trajectory tracking of steering and diving plane of AUV.

References:

[1] Anderson, B.D.O. and J.B. Moore, Optimal Control: Linear Quadratic Methods, Englewood Cliffs, NJ: Prentice-Hall, 1990.

[2] J.A. Primbs, V. Nevistic and J.C. Doyle, “Nonlinear optimal control: a control Lyapunov function and receding horizon perspective”, Asian Journal of Control, Vol.1, pp. 14-24, 1999.

[3] C.H. Won and S. Biswas, “Optimal control using an algebraic method for control-affine nonlinear systems”, International Journal of Control, Vol80, No. 9, pp. 1491-1502, September, 2007.

[4] B.V. Dasarathy, “optimal control in nonlinear system”, correspondence of IEEE Transaction on automatic control, pp. 690-691, December, 1970.

[5] J.D. Pearson, “Approximation methods in optimal control”, Journal of Electronics and Control, Vol. 13, pp. 453-469, 1962.

[6] Byrnes CI, Isidori A, Willems JC.1991. “Passivity, feedback equivalence, and the global stabilization of minimum phase nonlinear systems,” IEEE Trans. Automat. Control, 36, No. 11, 1228–1240.

[7] Efimov DV. 2002. “A condition of CLF existence for affine systems,” In: Proc. 41th IEEE Conf. Decis. Control,pp. 1882–1887.

[8] Faubourg L, Babtister J.1999. “Design of control Lyapunov functions for ‘Jurdjevic–Quinn’ systems,” In: The 1st EC–TMR Nonlinear Control Network Workshop.

[9] Freeman RA, Kokotovic PV. 1996. “Robust Nonlinear Control Design State Space and Lyapunov Techniques,” Birkh¨auser.

[10] Krstic M, Kanellakopoulos I, Kokotovic PV.1995. “Nonlinear and Adaptive Control Design”, John Wiley and Sons.

[11] Sontag ED.1989. “A universal construction of Artstein’s theorem on nonlinear optimization,” Syst. Control Lett., 13, 117–123.

[12] Primbs JA, Nevistic V, Doyle JC.2000. “A receding horizon generalization of pointwiseminnorm controllers,” IEEE Trans. Automat.Control, 45, No. 5.

[13] Shahmansoorian, A. (2009). Inverse optimal control and construction of control Lyapunov functions. Journal of Mathematical Sciences J Math Sci,161(2), 297-307. doi:10.1007/s10958-009-9553-5.

[14] R. E. Kalman, “When is a linear control system optimal?,” ASME Journal of Basic Engineering, pp. 51–60, March 1964.

[15] J. N. Tsitsiklis and M. Athans, “Guaranteed robustness properties of multivariable nonlinear stochastic optimal regulators,” IEEE Transactions on Automatic Control, vol. 29, no. 8, pp. 690–696, August 1984.

[16] S. Torkel Glad, “On the gain margin of nonlinear and optimal regulators,” IEEE Transactions on Automatic Control, vol. 29, no. 7, pp. 615–620, July 1984.

[17] S. Torkel Glad, “Robustness of nonlinear state feedback–a survey,” Automatica, vol. 23, no. 4, pp. 425–435, 1987.

[18] R. A. Freeman and P. V. Kokotovic, “Optimal nonlinear controllers for feedback linearizable systems,” in Proceedings of the American Control Conference, Seattle, Washington, June 1995, pp. 2722–2726.

[19] R. Sepulchre, M. Jankovic, and P. Kokotovic, Constructive Nonlinear Control, Communication and Control Engineering Series.Springer-Verlag, 1997.

[20] B. Hamzi, “Some results on inverse optimality based designs,” Systems Control Letters, vol. 43, pp. 239–246, 2001.

[21] Krstic, M., and P. Tsiotras. "Inverse Optimal Stabilization of a Rigid Spacecraft."IEEE Transactions on Automatic Control IEEE Trans. Automat. Contr. 44.5 (1999): 1042-049. Web. 16 July 2016.

[22] Shahmansoorian, Aref, B. Moshiri, A. Khaki Sedigh, and S. Muhammadi. "Inverse Optimal Controller Design Using CLFs Obtained from Feedback Linearization." Proceedings of 2005 CACS Automatic Control Conference Tainan, Taiwan, Nov 18-19, 2005. IEEE: n.p., 2005. Web. 17 May 2016.

[23] Khalil HK, Saberi A. Adaptive stabilization of a class of nonlinear systems using high-gain feedback. IEEE Transactions on Automatic Control 1987; AC-32 (11):1031–1035.

[24] Saberi A, Sannuti P. Observer design for loop transfer recovery and for uncertain dynamical systems. IEEE Transactions on Automatic Control 1990; 35 (8):878–897.

[25] Tornambe A. Use of asymptotic observers having high gains in the state and parameter estimation. Proceedings of IEEE Conference on Decision and Control , Austin, Texas, 1988; 1791–1794.

[26] Esfandiari F, Khalil HK. Observer-based design of uncertain systems: recovering state feedback robustness under matching conditions. Proceedings of Allerton Conference , Monticello, IL, September 1987; 97–106.

[27] Gauthier JP, Hammouri H, Othman S. A simple observer for nonlinear systems application to bioreactors. IEEE Transactions on Automatic Control 1992; 37(6):875–880.

[28] Besançon G. High-gain observation with disturbance attenuation and application to robust fault detection. Automatica 2003; 39 :1095–1102.

[29] Busawon K, Farza M, Hammouri H. Observer design for a special class of nonlinear systems. International Journal of Control 1998; 71 :405–418.

[30] Deza F, Busvelle E, Gauthier JP, Rakotopara J. High gain estimation for nonlinear systems. System & Control Letters 1992; 18 :295–299.

[31] Gauthier JP, Kupka IAK. Observability and observers for nonlinear systems. SIAM Journal on Control and Optimization 1994; 32 :975–994.

[32] Hammouri H, Targui B, Armanet F. High-gain observer based on a triangular structure. International Journal of Robust and Nonlinear Control 2002; 12 :497–518.

[33] Viel F, Busvelle E, Gauthier JP. Stability of polymerization reactors using I/O linearization and a high-gain observer. Automatica 1995; 31 :971–984.

[34] Esfandiari F, Khalil HK. Output feedback stabilization of fully linearizable systems. International Journal of Control 1992; 56 :1007–1037.

[35] Mita T. On zeros and responses of linear regulators and linear observers. IEEE Transactions on Automatic Control 1977; AC-22 (3):423–428.

[36] Polotskii VN. On the maximal errors of an asymptotic state identifier. Automation and Remote Control 1979; 11 :1116–1121.

[37] Andrieu V, Praly L, Astolfi A. High gain observers with updated gain and homogeneous correction terms. Automatica 2009; 45 (2):422–428.

[38] Alvarez-Ramirez J, Fermat R. Robust PI stabilization of a class of chemical reactors. System & Control Letters 1999; 38 :219–225.

[39] Byrnes CI, Celani F, Isidori A. Omega-limit sets of a class of nonlinear systems that are semiglobally practically stabilized. International Journal of Robust and Nonlinear Control 2005; 15 :315–333.

[40] Gonzalez-Trejo J, Alvarez Ramirez J, Fernandez G. Robust control with uncertainty estimation for feedback linearizable systems: application to control of distillation columns. Journal of Process Control 1999; 9 :221–231.

[41] Imsland L, Findeisen R, Bullinger E, Allgower F, Foss BA. A note on stability, robustness and performance of output feedback nonlinear model predictive control. Journal of Process Control 2003; 13 :633–644.

[42] Khalil HK, Esfandiari F. Semiglobal stabilization of a class of nonlinear systems using output feedback. IEEE Transactions on Automatic Control 1993; 38 (9):1412–1415.

[43] Oh S, Khalil HK. Nonlinear output feedback tracking using high-gain observer and variable structure control. Automatica 1997; 33 :1845–1856.

[44] Khalil HK. Robust servomechanism output feedback controllers for a class of feedback linearizable systems. Automatica 1994; 30 (10):1587–1599.

[45] Khalil HK. On the design of robust servomechanisms for minimum-phase nonlinear systems. International Journal of Robust and Nonlinear Control 2000; 10 :339–361.

[46] Mahmoud NA, Khalil HK. Asymptotic regulation of minimum phase nonlinear systems using output feedback. IEEE Transactions on Automatic Control 1996; 41 (10):1402–1412.

[47] Atassi AN, Khalil HK. A separation principle for the stabilization of a class of nonlinear systems. IEEE Transactions on Automatic Control 1999; 44 :1672–1687.

[48] Adeely, Usman, Adeel A. Zaidiz, and Attaullah Y. Memon. "Path Tracking of a Heavy Weight Torpedo in Diving Plane Using an Output Feedback Sliding Mode Controller."2015 12th

International Bhurban Conference on Applied Sciences and Technology (IBCAST) (2015): n. pag. Web. 17 July 2016.

[49] Thor I. Fossen Book “Guidance and Control of Ocean Vehicle”. 1994.

[50] F. Esfandiari, H.K.K., Output feedback linearization of fully linearizable sytems. International Journal of Control, 1992. 56: p. 31.

[51] Khalil, H. (2002). Nonlinear systems.3rd Edition. Upper Saddle River, N.J.: Prentice Hall Chapter 4.

[52] SNAME (1950). The Society of Naval Architects and Marine Engineers. Nomenclature for Treating the Motion of a Submerged Body through a Fluid, Technical and Research Bulletin No. 1-5.

[53] Cyrille Vuilmet, High order sliding mode control applied to a heavy weight torpedo, Proceedings of the IEEE conference on control applications, Toronto, Canada, 2005.

[54] Anderson, B.D.O. and J.B. Moore, Optimal Control: Linear Quadratic Methods, Englewood Cliffs, NJ: Prentice-Hall, 1990.

[55] Nonlinear Systems. Third Edition by Hassan K. Khalil. Page#531.

[56] Usman Adeel, Adeel A. Zaidi, and Attaullah Y. Memon, Path tracking of heavy weight torpedo in diving plane using an output feedback sliding mode controller, IEEE international Bhurban conference on applied sciences and technologies (IBCAST), 2015.

[57] Theorem 14.3 and Corollary 14.1 of Nonlinear System by Hassan K. Khalil. Page No. 584-585.

[58] Sontag ED.1989. “A universal construction of Artstein’s theorem on nonlinear optimization,” Syst. Control Lett., 13, 117–123.

[59] Freeman RA, Kokotovic PV. 1996. “Robust Nonlinear Control Design State Space and Lyapunov Techniques, ”Birkh¨auser.

[60] Mahmoud NA, Khalil HK. Asymptotic regulation of minimum phase nonlinear systems using output feedback. IEEE Transactions on Automatic Control 1996; 41 (10):1402–1412.

Appendix A

A.1 Nominal Hydrodynamic and Physical parameters of AUV

Model and Hydrodynamic Parameters	**Values**
Z_w	66.6
M_w	30.7
Z_q	-9.67
M_q	-6.87
Added mass coefficients	
$Z_{\dot{w}}$ Cross flow added mass	-35.5Kg
$M_{\dot{q}}$ Cross flow added mass	$-4.88 Kg.m^2/rad$
$X_{\dot{u}}$ Axial added mass	-0.93Kg
Z_{uw}	-28.6 Kg/m
$Z_{\|w\|w}$	-131 Kg/m
$Z_{q\|q\|}$	$-0.632 Kg.m/rad^2$
$M_{\dot{w}}$	-1.93 Kg.m
General vehicle and environmental parameters	
I_y Vehicle moment of inertia around y-axis	$3.45 Kg.m^2$
M	30.48 Kg
Control surface nonlinear coefficients	
$Z_{uu\delta}$ Lift coefficient for elevator displacement	-6.15 Kg/(m·rad)
$M_{uu\delta}$ Pitch moment coefficient for elevator displacement	6.15Kg/rad
Vehicle Speed	
u	2 m/s

A.2 Variables values used in expressions

$$A_{31} = \frac{Z_w}{m - Z_{\dot{w}}}$$

$$A_{32} = \frac{mu - X_{\dot{u}}u + Z_q}{m - Z_{\dot{w}}}$$

$$B_{31} = \frac{Z_{uu\delta_s}}{m - Z_{\dot{w}}}$$

$$A_{41} = \frac{M_w}{I_y - M_{\dot{q}}}$$

$$A_{42} = \frac{M_q}{I_y - M_{\dot{q}}}$$

$$B_{41} = \frac{M_{uu\delta_s}}{I_y - M_{\dot{q}}}$$

$C_1=B_{41}/B_{31}$

$C_2=C_1*u$

$C_3=B_{41}$

$C_4= (A_{31}/B_{31})-(A_{41}/B_{41}) + ((A_{32}*B_{41})/ (B_{31})^2)-(A_{42}/B_{31})$

$C_5=C_4*u$

$C_6= ((A_{32}*B_{41})/B_{31})-A_{42}$

$C_7=A_{31}+ ((A_{32}*B_{41})/B_{31})$

$C_8= (A_{31}*u) + ((A_{32}*B_{41})/B_{31})-((B_{41}*(u^2))/B_{31})$

$C_9= (B_{41}*u)-(A_{32}*B_{41})$

$C_{10}=B_{41}*u$

$C_{11}= (B_{41}*(u^2))/B_{31}$

$C_{12}= (2*B_{41}*u)/B_{31}$

$C_{13}=B_{41}$

$C_{14}=B_{41}/B_{31}$

$C_{15}=B_{31}$